Chapter -5: *In silico* multi-target fishing, docking and molecular dynamics simulation studies of acyl and aldehyde pyrazolones, o- vanillin and some of their novel Schiff bases

5. *In silico*multi-target fishing and docking and molecular dynamics simulation studies of acyl and aldehyde pyrazolones, o- vanillin and some of their novel Schiff bases

5.1 INTRODUCTION

Acceleration in Bioinformatics and Cheminformatics hoarded a huge amount of protein sequence and chemical structure data from sequencing centres and synthetic chemistry laboratories all over the globe in private and public repositories on World Wide Web. Before the advent of interdisciplinary computational areas, identification of targeted therapeutic compounds faced an obstacle of "Price and Period". In the year 1980, Life Science community witnessed a high throughput and virtual screening of chemical compounds against protein and nucleic acids targets, widely accelerating the process of structure based drug discovery while chemists still faced the challenge of devising as much chemical compounds for Biologists. After 1990, many chemical-diversity-related approaches like structural descriptor computations, structural similarity algorithms, classification algorithms, diversified compound selections, and library enumerations were developed. Further the filtering techniques to discriminate toxic and non-toxic compounds were developed alongside the Cheminformatics timeline[374-377].

The current medicinal chemistry research moves from single to multi-target approach, which is called polypharmacology. It is relatively difficult to chemicallyachieve a single target specificity. Furthermore, it is now evidentthat many of the most effective drugs in therapeutic areas asdiverse as oncology (such as Gleevec), psychiatry (such as serotoninreuptake inhibitors), and inflammation (such as aspirin) actupon multiple rather than a single target[378-381]. Computational target fishing is another approach where the ligand information is available but the biological target is not known. Through this approach, it is possible to predict the mechanism of action of small molecules by identifying their interacting proteins. Computational target fishing employs various chemoinformatics tools, databases, and machine learning algorithms[382-384]. Various previous studies show the prediction of multi-target small molecules [385-389] through target fishing [390, 391]. The current study is focused on the prediction of biological target through target fishing approach for the novel acyl and aldehyde pyrazolones,o- vanillin and some of their

novel Schiff baseswhich are synthesized by our group [392-394].The obtained results were confirmed via docking and molecular dynamics simulation studies.

5.2 MATERIALS AND METHODS

The synthesised threeacyl pyrazolone, four aldehyde pyrazolone and seven O-vanillin chemical molecules were used to carry out this Cheminformatics study. The list of molecules with two dimensional structuresare shown in figures5.1 and 5.2.

Figure 5.1: Two dimensional structures of acyl and aldehyde pyrazolones

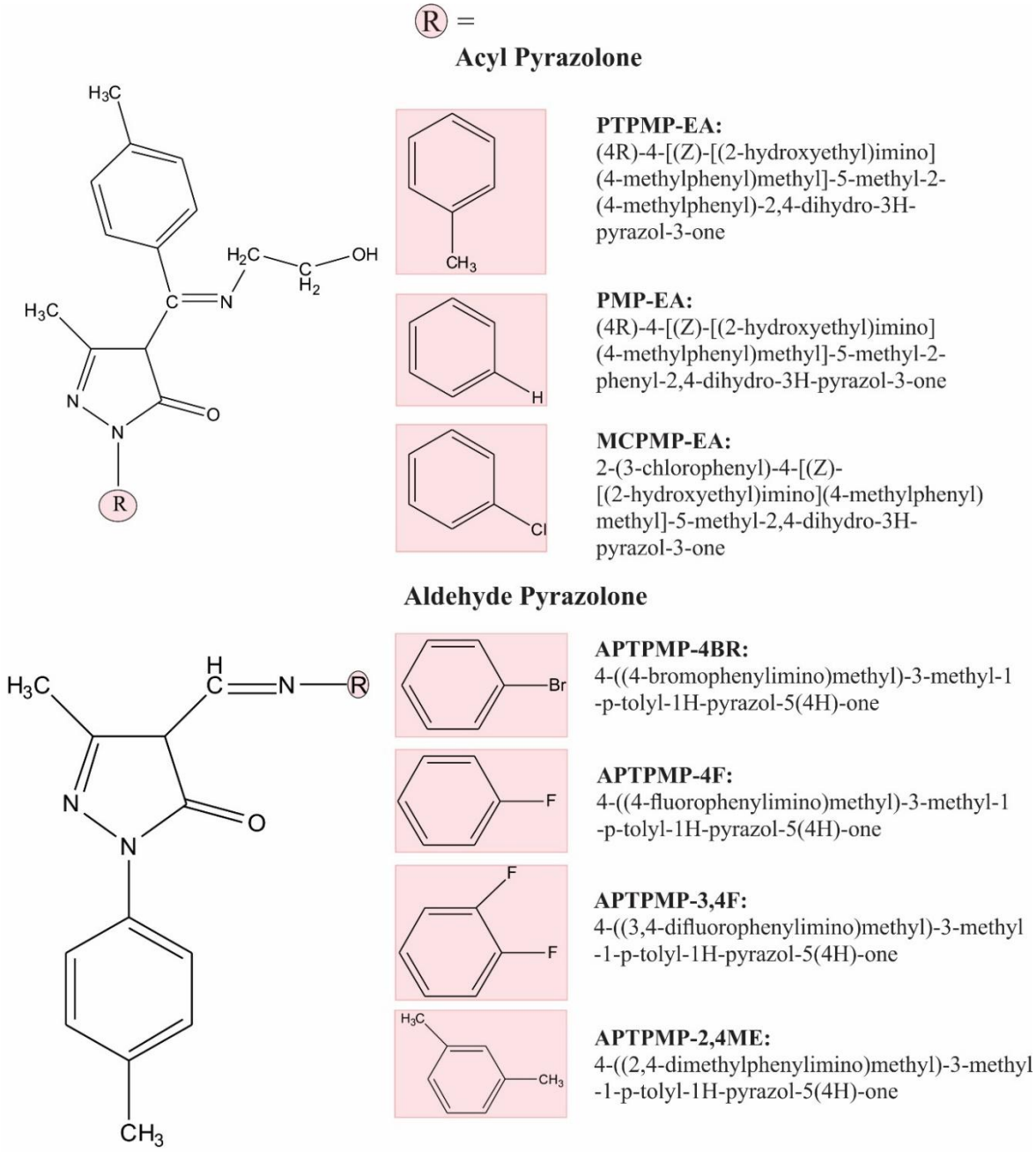

Figure 5.2: Two dimensional structures of o-vanillin

O-Vanillin

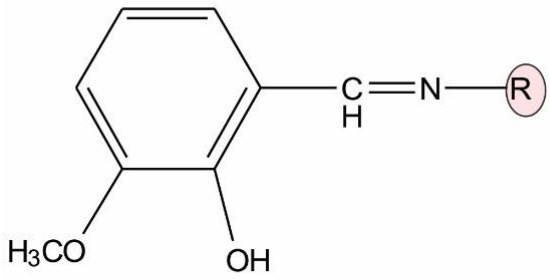

R =

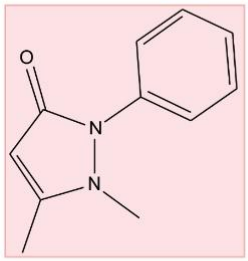

V-4AAP:
4-(2-hydroxy-3-methoxybenzylideneamino)
-1,2-dihydro-2,3-dimethyl-1-phenylpyrazol-
5-one

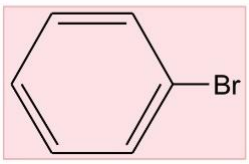

V-4BR:
2-((4-bromophenylimino)methyl)-6
-methoxyphenol

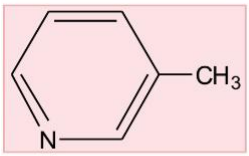

MMM:
2-((5-methylpyridin-2-ylimino)
methyl)-6-methoxyphenol

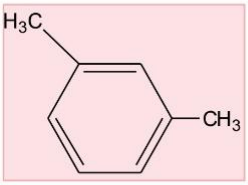

V-2,4ME:
2-((2,4-dimethylphenylimino)methyl)-6
-methoxyphenol

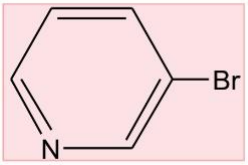

BMM:
2-((5-bromopyridin-2-ylimino)methyl)
-6-methoxyphenol

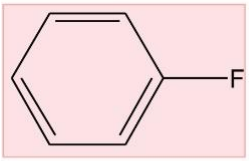

V-4F
2-((4-fluorophenylimino)methyl)
-6-methoxyphenol

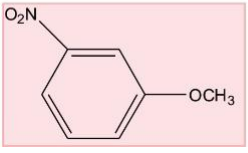

V-2N4A
2-((4-methoxy-2-nitrophenylimino)
methyl)-6-methoxyphenol

5.2.1 Ligand Preparation

All Molecules were prepared by using LigPrep module of Schrodingerwhich performs addition of hydrogens, 2D to 3D conversion, rectifies bond lengths and bond angles, andconverts to minimum energy structure with correct chiralities, ionization states, tautomers, stereochemistry and ring conformations[395].

5.2.2 Drug likeliness property prediction

The drug likeliness of prepared molecules were performed by QikPropmodule of Schrodinger which rapidly screens compounds by predicting a wide variety of relevant properties such as LogP, HERG, MDCK, Lipinski's rule of 5 and many others[396]. Molecules passing the QikProp properties were exported and taken for further analysis.

5.2.3 Toxicity Prediction

Toxicity prediction is a phenomenon that involves potential adverse drug effect on a range of biological functions which provide a heavy evidence on toxicity of untested chemical compounds. ToxPredict tool was used to predict the toxicity level of all the molecules [http://apps.ideaconsult.net:8080/ToxPredict]. ToxPredict predicts and reports on toxicities including several parameters such as carcinogenicity, mutagenicity, human toxicological hazards and other 20 parameters [397].

5.2.4 Biological function prediction

Protein targets and biological activity for screenedmolecules from previous steps were predicted using diverse range of publicly available Bioinformatics and Cheminformatics tools and databases. Due to limitation in the accuracy of each tool we rely on various tools to get more accurate result.

The first resource used was Therapeutic Target Database (TTD) [http://bidd.nus.edu.sg/group/cjttd/] to obtain the drugs similar to the query compounds, keeping "tanimoto coefficient" score till 0.85. TTD is a constantly updated database incorporating information on the subject of potential targets and the corresponding approved, clinical trial and analytical drugs. It also contains more than 2300 targets, which includes 388 successful and 461 clinical trial targets, 20600

drugs, which includes 2003 approved and 3147 clinical trial drugs, 20,000 multitarget agents against almost 400 target-pairs and the activity data of 1400 agents against 300 cell lines [398].

The second resource used isSuperTarget, a resource that explores drug-target relationship information about drug discovery indication areas [http://bioinf-apache.charite.de/supertarget_v2/]. A list of protein targets with excellent similarity of 0.9 was obtained by SuperTarget[399].

The third resource used isSTITCH,which has been developed to provide comprehensive protein chemical interaction information from various metabolic pathways, crystal structures and binding experiments[http://stitch.embl.de/]. The predicted functional interaction partners were obtained by STITCH[400].

The fourth resource is ChemMapper [http://lilab.ecust.edu.cn/chemmapper/], a free web server for computational drug discovery based on the concept that compounds sharing high 3D similarities may have relatively similar target association profile. It integrates more than 305000 chemical structures with pharmacology annotations,from commercial and public chemical catalogueswhich includes BindingDB, chEMBL, DrugBank, Kyoto Encyclopedia of Genes and Genomes (KEGG), Protein Data Bank (PDB). In-house SHAFTS method which combines the strength of molecular shape superposition and chemical feature matching is used in ChemMapper to perform the 3D similarity searching, ranking, and superposition. The query molecules alignswith each target compound in the database and calculates the 3D similarity scores and the top most similar structures are returned. Based on this result a chemical-protein network is constructed and a random walk algorithm is taken to compute the probabilities of the interaction between the query structure and proteins which are associated with hit compounds. These potential protein targets are ranked by the standard score of the probabilities. ChemMapper can be useful in a variety of polypharmacology, drug repurposing, chemical-target association, virtual screening, and scaffold hopping studies[401]. The protein target which hit with score value one is considered from ChemMapper.

All the above performed resources execute similarity search based on the input structure of ligand molecules. Pharmacophore based similarity search is a new method to find similar molecules and its targets with higher accuracy. Pharmacophore is defined as a 3D structural feature that illustrates the interaction of a ligand molecule

with a target receptor in a specific binding site [402]. To achieve this, the PharmMapper is used. It is an online target identification tool based on pharmacophore mapping [http://59.78.96.61/pharmmapper/]. It has large, in-house repertoire of pharmacophore database extracted from all the targets in TargetBank, DrugBank, BindingDB and Potential Drug Target Database (PDTD). Over 7,000 receptor-based pharmacophore models are stored and accessed by PharmMapper. PharmMapper finds the best mapping poses of the query molecules against all the targets in PharmTargetDB and top potential drug targets as well as respective molecule's aligned poses obtained with z-score. The z-score greater than three was considered as a final molecule as the greater z-score are highly significant [403].

Enormous manual analysis was carried to obtain highly accurate and consensus final protein targets for each ligand molecule from all tools.

5.2.5 Protein structure retrieval

Thethree dimensional structure of finalizedproteins which probably bind with the selected ligand molecules were obtained from Protein data Bank (PDB) along with its co crystalized inhibitor (Reference Ligand) [http://www.rcsb.org/pdb/home/home.do][404].

5.2.6 Approved drugs and Inhibitor retrieval

The available approved drugs and inhibitors of each target were used for the comparative analysis in docking procedure. The approved / experimental drugs for the proteins, which finalized from the previous steps were retrieved from DrugBank [www.drugbank.ca]. DrugBank is a comprehensive, high-quality, freely accessible, online database containing information on drugs and drug targets[405]. The inhibitors for each target were obtained from chEMBL [https://www.ebi.ac.uk/chembl/]. ChEMBL is a database of bioactive drug-like small molecules, it contains small molecule structures, calculated properties (e.g. logP, Molecular Weight, Lipinski Parameters, etc.) and abstracted bioactivities (e.g. binding constants, pharmacology and ADMET data)[406].

5.2.7 Protein-Ligand Docking and Visualization of results

The protein-ligand interactionswere further confirmed by protein-ligand docking with theobtained proteins from the above steps and the respective chemical molecules. The molecular docking studies were carried out for all proteins separately with their respective synthesised molecule, approved / experimental drugs, inhibitors obtained from chEMBL, and reference ligand which isnaturally present in PDB structure of protein using Molegro Virtual Docker (MVD). It has two docking search algorithms: MolDock Optimizer and MolDock Simplex Evolution (SE). MolDock Optimizer is the default search algorithm in MVD. In order to dock the receptor and ligand, the receptor was prepared from the "prepare molecule" option provided. Then, for grid searching, cavities were generated using the "detect cavity" option. Finally, the ligands and the targets obtained from the previous steps were provided in an sdf file format for docking using the docking wizard. During docking, the following parameters were fixed: number of runs 10, population size 50, crossover rate 0.9, scaling factor 0.5, maximum iteration 2,000, and grid resolution 0.30 [407]. The obtained results were analysed in comparison with an already reported inhibitors.

The software Pymol andMolegro Virtual Docker (MVD) were used to visualize the docked result. PyMOL is a powerful and comprehensive molecular visualization product for rendering and animating 3D molecular structures [http://www.pymol.org/pymol]. Molegro Virtual Docker is an integrated platform for predicting protein-ligand interactions. Molegro Virtual Docker handles all aspects of the docking process from preparation of the molecules to the determination of the potential binding sites of the target protein and prediction of the binding modes of the ligands[407].

5.2.8 Molecular dynamics simulation studies

Molecular dynamics (MD) simulations are important tools for understanding the physical basis of the structure and function of biological macromolecules. The early view of proteins as relatively rigid structures has been replaced by a dynamic model in which the internal motions and resulting conformational changes play an essential role in their function. The atoms and molecules are allowed to interact for a fixed period of time, giving a view of the dynamical evolution of the system. In the most common version, the trajectories of atoms and molecules are determined by numerically solving Newton's equations of motion for a system of interacting

particles, where forces between the particles and their potential energies are calculated using interatomic potentials or molecular mechanics force fields[408].The MD simulations of best docked complexes wereperformed using a Desmond Molecular Dynamics module of Schrodinger, with Optimized Potentials for Liquid Simulations (OPLS) all-atom force field 2005 [409, 410]. The complexes were prepared before simulation by the protein preparation wizard. Prepared protein-ligand complexes were then solvated with an SPC water model in a triclinic periodic boundary box. To prevent interaction of the protein complex with its own periodic image, the distance between the complex and the box wall was kept 10 Å. The energy of the prepared systems was minimized for 5000 steps using the steepest descent method or until a gradient threshold of 25 kcal/mol/Å was achieved. It was followed by L-BFGS (Low-memory Broyden- FletcherGoldfarbShanno quasi-Newtonian minimiser) until a convergence threshold of 1 kcal/mol/Å was met. For system equilibration, the default parameters in Desmond were applied. The equilibrated systems were then used for simulations at a temperature of 300 K and a constant pressure of 1atm, with a time step of 2fs. For handling long range electrostatic interactions Smooth Particle Mesh Ewald method was used, whereas Cutoff method was selected to define the short range electrostatic interactions. A cut-off of 9 Å radius was used. The system is allowed to run up to 20 nanoseconds (ns) to observe the better performance of the protein-ligand complex.

5.3 RESULTS AND DISCUSSION

5.3.1 Ligand Preparation, Drug likeliness and Toxicity Prediction

The drug likeliness of prepared molecules was performed by QikPropmodule of Schrodinger. ToxPredict tool was used to predict the toxicity level of all the molecules. The result of these three tools revealed that all three molecules of acyl pyrazolone,four molecules of aldehyde pyrazolone and seven molecules of O-Vanillin pass the drug likeliness and toxicity prediction.

5.3.2 Biological function prediction

Biological function prediction was carried out by similarity search for the synthesized molecules of pyrazolone and o-vanillin and their derivatives against drug, drug-like, small molecules and target database. Results of all the databases and tools

were compared with each other to find accurate and consensus targets. Finally, the obtained targetswere tabulated in table 5.1 and 5.2 with their detailed information, which includes PDB code andthe disease involved.In all, five, threeand fourbiological targets were predicted for acyl and aldehyde pyrazolones, and o-vanillin respectively. Out of these, the protein RNA dependent RNA polymerase interact with both acyl pyrazolone and o-vanillinand their derivatives (Schiff bases).

Table 5.1 Summaryof predicted target proteins for the acyl and aldehyde pyrazolone; and its involved mechanism / disease

S.No	Name of predicted target	PDB ID	Mechanism/ Disease involved
	Acyl pyrazolone		
1.	Caspase-1 (Interleukin-1 beta converting enzyme)	1BMQ	Cancer & Anti-inflammatory
2.	Tyrosine-protein phosphatase non-receptor type 1	1Q6N	Diabetes
3.	Genome polyprotein (RNA Polymerase)	1YVX	Hepatitis C Virus
4.	HIV-1 Protease	1HXW	HIV
5.	Estrogen sulfotransferase	1G3M	Inactivation of estrogens
	Aldehyde pyrazolone		
1.	Class 2 dihydroorotate dehydrogenase, mitochondrial	1D3H	Autoimmune diseases, Immunosuppression, Cancer
2.	Heat shock protein HSP 90-alpha	1UY6	Cancer
3.	Proto-oncogene tyrosine-protein kinase LCK	3BYS	Cancer

Table 5.2Summary of predicted target proteins for the O-Vanillin; and its involved mechanism / disease

S.No	Name of predicted target	PDB ID	Mechanism/ Disease involved
1.	Orotidine 5-phosphate decarboxylase	1LP6	Rate limiting step for Methane production
2.	Prothrombin	3C1K	Prevent Blood coagulation
3.	RNA dependent RNA polymerase	1YVX	Hepatitis C Virus
4.	Androgen receptor	1E3G	Cancer

The acyl pyrazolone PTPMP-EA predicted Caspase-1 (Interleukin-1 beta converting enzyme) as its target. Caspase-1 is a promising drug target for various cancers and inflammatory disease [411-413]. Minocycline (DrugBank accession Number: DB01017) is the only approved drug available but, many experimental drugs are available for this target.

HIV-1 protease and Tyrosine-protein phosphatase non-receptor type 1 (PTP1B) of humanswere predicted as a target for acyl pyrazolone PMP-EA. HIV-1 protease is a retroviral aspartyl protease (retropepsin) that is essential for the life-cycle of HIV, the retrovirus that causes acquired immune deficiency syndrome (AIDS) [414]. As this protein is a prime target for drug therapy, several inhibitors have been licensed. However, due to the high mutation rates in its active site HIV developed resistance[415]. PTP1B has been implicated in the regulation of the insulin signaling pathway and represents an attractive target for the design of inhibitors in the treatment of type 2 diabetes and obesity [416-418]. Though it has more than 50 experimental drugs, only one approved drug tiludronate (DrugBank accession Number: DB01133) is available.

Genome polyprotein (RNA polymerase) of Hepatitis C Virus(HCV) were predicted as a target for acyl pyrazolone PMP-EA and vanillin V-4BR. It is RNA dependent RNA polymerase, which replicating the HCV's viral RNA by using the viral positive RNA strand as its template and catalyzes the polymerization of ribonucleoside triphosphates (rNTP) during RNA replication [419, 420]. Hindering the activity of RNA polymerase terminate the proliferation of Hepatitis C virus. Many

inhibitors are available for this protein, but suitable drug molecules are under clinical trial [421, 422].

The acyl pyrazolone MCPMP-EA predicted estrogen sulfotransferase as its target. Estrogen sulfotransferase is a cytosolic enzyme that catalyzes the sulfoconjugation and inactivation of estrogens by making it more soluble. However, sulfonated estrogenhas a long half-life, so they act as storehouses. When needed, they are readily converted to active estrogens by removal of the sulfate by a sulfatase enzyme. The sulfotransferases and sulfatases that act on estrogen are attractive targets for cancer therapy since some breast cancer cells require a steady supply of estrogen for growth [423, 424]. Acetaminophen and Cyclizine (DrugBank accession Number DB00316 and DB01176 respectively) are the two approved drugs available to control estrogen sulfotransferase activity.

Class 2 dihydroorotate dehydrogenase (EC 1.3.5.2) is an enzyme that contains flavin mononucleotide (FMN) which is found in the mitochondrial membrane of eukaryotes. This catalyzes the fourth step in the de novo biosynthesis of pyrimidine (KEGG Pathway map: map00240) [http://www.genome.jp/kegg/pathway.html]. It converts dihydroorotate to orotate[425]. As rapidlyproliferating human T cells have an exceptional requirement for de novopyrimidine biosynthesis, small molecule DHODH inhibitors constitute anattractive therapeutic approach to autoimmune diseases, inflammatory diseases, multiple sclerosis, and cancer[426]. Two such inhibitors, brequinar (BRE) and leflunomide (LEF), have proven effective as drugs against various cancers and rheumatoid diseases [427, 428]. Through target fishing approach the molecule aldehyde pyrazoloneAPTPMP-4BR, APTPMP-4F, APTPMP-3,4F and APTPMP-2,4ME were predicted as its target.

The proto-oncogene tyrosine-protein kinase–lymphocyte cell kinase (LCK) is the lymphocyte-specific protein which belongs to the member of the Src family of protein tyrosine kinases [429]. Inhibiting this kinase protein will be a remedy for T-cell-mediated autoimmune and inflammatory disease, colon cancer and leukemia. Leukemia is a type of cancers that begins in the bone marrow and results in high numbers of abnormal white blood cells [430-433]. Dasatinib (DrugBank accession Number: DB01254) is the only approved drug available for this target. The aldehyde pyrazolone APTPMP-4BRis now predicted as targeting this protein.

The cytosolic heat shock protein HSP 90-alpha (Hsp90α) was predicted as a target for an aldehyde pyrazolone APTPMP-4F. Hsp90α overexpresses in cancer cells and it acts as a protector of less stable proteins produced by DNA mutations [434, 435]. Hence, Hsp90α is a potential drug target for cancer therapy [436]. Rifabutin and Nedocromil (DrugBank Accession Number: DB00615 and DB00716 respectively) are the approved drugs available for this target.

Vanillin V-4BR predicted Orotidine 5-phosphate decarboxylase (ODCase) of Methanobacteriumthermoautotrophicum (Archaea) as its target. Itcatalyzes the last step in the de novo pyrimidine biosynthesis pathway, converting OMP to UMP, which in turn serves as the source of all cellular pyrimidine nucleotides. ODCase continues to elicit keen interest not only because of its obvious importance in DNA and RNA synthesis, but also in cell growth and proliferation. In Methanobacteriumthermoautotrophicum, controlling this enzyme is a rate limiting step for Methane production[437]. It does not have any inhibitors in the available chemical databases.

Prothrombin (coagulation factor II) is predicted as the target for vanillin MMM and V-2,4ME. Prothrombin is proteolytically cleaved to form thrombin in the coagulation cascade, which ultimately results in the reduction of blood loss[438, 439]. Inhibition of prothrombin prevent blood coagulation, which is essential for many biochemical experiments and surgical procedures. Six approved drugs and many hundreds of inhibitors are available to deactivate prothrombin.

Vanillin MMM predicted Androgen receptor (AR) also known as NR3C4 of humans as its target. It is activated by binding of either of the androgenic hormones testosterone or dihydrotestosterone[440]. Although AR is involved in many physiological function, it is a critical mediator of prostate cancer promotion [441, 442]. More than 21 approved and 23 experimental drugs are targeting Androgen receptor [405].

5.3.3 Protein structure retrieval,Protein-Ligand Docking andVisualization

The three dimensional structures of all proteins listed in table 5.1 and 5.2 were retrieved from Protein Data Bank (PDB)

The protein-ligand interactions were further confirmed by protein-ligand docking by MVD to obtain better results. Docking results with energy valuesof acyl,

aldehyde pyrazolone and O-Vanillin are shown in the tables5.3, 5.5 and 5.7 and the active site amino acid residues along with the number of hydrogen bond and its energy (kcal/mol) are shown in tables5.4, 5.6 and 5.8 respectively.The screenshot of docking results of acyl pyrazolone shown in figures5.3, 5.4 and 5.5, aldehyde pyrazolone is given in figures5.6, 5.7, 5.8 and 5.9, and those of o-vanillin in figures5.10, 5.11 and 5.12.

Docking result of acyl pyrazolone PTPMP-EA with Caspase-1 (Interleukin-1 beta converting enzyme) (PDB ID: 1BMQ) shows better docking score (-107.65 kcal/mol) than already available approved drug Minocycline (DrugBank ID: DB01017) [443] (-74.55 kcal/mol) but co-crystal(reference ligand) inhibitor (3S)-N-methanesulfonyl-3-[[1-[N-(2-naphthoyl)-L-valyl]-L-prolyl]amino]- 4-oxobutanamide shows better docking energy [444]than PTPMP-EA but it's failed to possess drug likeliness property. The active site amino acid residues Pro 177, Arg 179, Ser 236, His 237, Gln283, Cys 285, Ser 339, Arg 341 and Pro 343 are responsible for the binding of PTPMP-EA with 8 hydrogen bonds and the hydrogen bonds energy (Binding energy) is -7.4 kcal/mol. Though approved drug having better binding energy (-15.5 kcal/mol) than PTPMP-EA, it fails to acquire best docking score than PTPMP-EA.

The binding energy has been calculated based on the following formula

Binding energy of ligand = Energy of complex - (Energy of protein + Energy of ligand)

This equation generates negative binding energy. Lower the negative energy, better the affinity.

The Root Mean Square Deviation (RMSD) of PTPMP-EA and approved drug is 3.9 Å. The RMSD is the square root of the mean of the square of the distances between the matched atoms.

$RMSD = SQRT[\{SUM(d_{ii})^2\}/N]$

where d_{ii} is the distance between the i^{th} atom of structure 1 and the i^{th} atom of structure 2 and N is the number of atoms matched in each structure. The analysis concludes that although the modified R-group of PTPMP-EA is not directly involved in the hydrogen bond interaction, it provides better docking score than already available approved drug for the inhibition of Caspase-1.

Table 5.3 Docking results of acyl pyrazolone, reference ligand, approved drug and inhibitors with their predicted targets

Query Molecule	Predicted Target	PDB ID	Mechanism/ Disease involved	Docking Energy (kcal/mol)					
				Respective Acyl Pyrazolone	Reference Ligand	Approved / Experimental Drug		Inhibitors from chEMBL	
						From	To	From	To
PTPMP-EA	Caspase-1 (Interleukin-1 beta converting enzyme)	1BMQ	Cancer & anti-inflammatory	**-107.65**	-164.50	-74.55	-	-178.17	-70.62
PMP-EA	Gag-Pol polyprotein (Protease)	1HXW	HIV	-123.35	-207.09	-197.95	-140.28	-206.39	-108.30
	Genome polyprotein (RNA Polymerase)	1YVX	Hepatitis C Virus	**-120.22**	-153.16	-123.48	-98.75	-142.01	-87.43
	Tyrosine-protein phosphatase non-receptor type 1	1Q6N	Diabetes	**-153.58**	-255.40	-90.42	-	-206.61	-28.91
MCPMP-EA	**Estrogen sulfotransferase**	**1G3M**	**Inactivation of estrogens**	**-131.72**	**-95.96**	**-92.10**	**-**	**-153.41**	**-141.44**

Table 5.4 Active site amino acid and hydrogen bond informationfrom docking results of acyl pyrazolone, reference ligand and approved drug

Query Molecule	Predicted Target	PDB ID	Respective Acyl Pyrazolone		Reference Ligand		Approved / Experimental Drug	
			No. of H Bonds & its energy (kcal/mol)	Active site Amino acid Residues	No. of H Bonds & its energy (kcal/mol)	Active site Amino acid Residues	No. of H Bonds & its energy (kcal/mol)	Active site Amino acid Residues
PTPMP-EA	Caspase-1 (Interleukin-1 beta converting enzyme)	1BMQ	8 (-7.4)	Pro 177, Arg 179, Ser 236, His 237, Gln 283, Cys 285, Ser 339, Arg 341, Pro 343	13 (-9.6)	Pro 177, Arg 179, His 237, Cys 285, Ser 339, Trp 340, Arg 341	10 (-15.5)	Pro 177, Arg 179, His 237, Gln 283, Ser 339, Trp 340, Arg 341, Pro 343, Arg 383
PMP-EA	Genome polyprotein (RNA Polymerase)	1YVX	7 (-6.0)	Thr 418, Ile 419, Arg 422, Met 423, Thr 476, Tyr 477, Lys 501, Trp 528	7 (-0.7)	Arg 422, Leu 474, Thr 476, Tyr 477, Arg 498, Trp 528	1 (0.0)	Ile 419, Arg 422, Met 423, His 475, Thr 476, Tyr 477, Lys 501, Trp 528
	Tyrosine-protein phosphatase non-receptor type 1	1Q6N	3 (-2.5)	Ala 517, Gln 521, Arg 1047, Asp 1048, Val 1049, Phe 1182, Ala 1217, Gly 1220, Arg 1221, Gln 1262	17 (-12.7)	Tyr 546, Arg 547, Asp 548, Phe 682, Cys 715, Ser 716, Ala 717, Ile 719, Gly 720, Arg 721, Gln 762, Ala 1018, His 1025, Glu 1026	17 (-12.7)	Tyr 1046, Val 1049, Asp 1181, Phe 1182, Cys 1215, Ser 1216, Ala 1217, Gly 1218, Ile 1219, Gly 1220, Arg 1221
MCPMP-EA	Estrogen sulfotransferase	1G3M	2 (-3.0)	Tyr 20, Phe 23, Pro 46, Phe 75, Phe 80, Phe 138, Phe 141, Val 145, Ala 146, His 148, Leu 242, Ile 246, Met 247,	3 (0.0)	Tyr 20, Lys 105, His 107, Val 145, Ala 146, Ile 246	0 (0.0)	Tyr 20, Phe 23, Pro 46, Phe 80, His 107, Phe 141, Val 145, Ala 146, His 148, Tyr168, Tyr

	Phe 254							239, Phe 254	

Table 5.5 Docking results of aldehyde pyrazolone, reference ligand, approved drug and inhibitors with their predicted targets

Query Molecule	Predicted Target	PDB ID	Mechanism/ Disease involved	Docking Energy (kcal/mol)					
				Respective Aldehyde Pyrazolone	Reference Ligand	Approved / Experimental Drug		Inhibitors from chEMBL	
						From	To	From	To
APTPMP-4BR	Class 2 dihydroorotate dehydrogenase, mitochondrial	1D3H	Autoimmune diseases, Immunosuppression, Cancer	**-136.64**	-113.64	-127.36	-	-153.56	-123.50
	Proto-oncogene tyrosine-protein kinase LCK	3BYS	Cancer	-123.48	-200.06	-165.98	-	-166.17	-96.94
APTPMP-4F	Class 2 dihydroorotate dehydrogenase, mitochondrial	1D3H	Autoimmune diseases, Immunosuppression, Cancer	**-143.85**	-113.64	-127.36	-	-153.56	-123.50
	Heat shock protein HSP 90-alpha	1UY6	Cancer	**-113.43**	-148.27	-130.31	-58.73	-192.39	-66.15
APTPMP-3,4F	Class 2 dihydroorotate dehydrogenase, mitochondrial	1D3H	Autoimmune diseases, Immunosuppression, Cancer	**-136.68**	-113.64	-127.36	-	-153.56	-123.50
APTPMP-2,4ME	**Class 2 dihydroorotate dehydrogenase, mitochondrial**	**1D3H**	**Autoimmune diseases, Immunosuppression,**	**-144.99**	**-113.64**	**-127.36**	**-**	**-153.56**	**-123.50**

Cancer

Table 5.6 Active site amino acid and hydrogen bond informationfrom docking results of aldehyde pyrazolone, reference ligand and approved drug

Query Molecule	Predicted Target	PDB ID	Respective Acyl Pyrazolone		Reference Ligand		Approved / Experimental Drug	
			No. of H Bonds & its energy (kcal/mol)	Active site Amino acid Residues	No. of H Bonds & its energy (kcal/mol)	Active site Amino acid Residues	No. of H Bonds & its energy (kcal/mol)	Active site Amino acid Residues
APTPMP-4BR	Class 2 dihydroorotate dehydrogenase, mitochondrial	1D3H	3 (-2.5)	Ala 96, Asn 145, Thr 283, Thr 285, Gly 306, Leu 309, Val 333, Gly 335, Val 336, Leu 355, Tyr 356, Thr 357, Ala 358	1 (-2.5)	Met 43, Pro 52, His 56, Ala 59, Thr 63, Phe 98, Met 111, Tyr 356, Leu359, Thr 360, Pro 364	6 (-6.01)	Pro 52, Ala 55, His 56, Arg 136, Val 143, Asn 145, Thr 285, Ser 305, Tyr 356, Thr 357, Thr 360
APTPMP-4F	Class 2 dihydroorotate dehydrogenase, mitochondrial	1D3H	3 (-4.56)	Ala 96, Asn 145, Thr 283, Thr 285, Gly 306, Leu 309, Val 333, Gly 335, Val 336, Leu 355, Tyr 356, Thr 357, Ala 358	1 (-2.5)	Met 43, Pro 52, His 56, Ala 59, Thr 63, Phe 98, Met 111, Tyr 356, Leu359, Thr 360, Pro 364	6 (-6.01)	Pro 52, Ala 55, His 56, Arg 136, Val 143, Asn 145, Thr 285, Ser 305, Tyr 356, Thr 357, Thr 360
	Heat shock protein HSP 90-alpha	1UY6	3 (0)	Asn 51, Ala 55, Ile 96, Gly 97, Met 98, Leu 107, Ala 111, Val 136, Phe	8 (0)	Ala 55, Leu 107, Ala 111, Phe 138, Tyr 139, Trp 162, Thr 184	8 (0)	Asn 51, Leu 107, Ile 110

			138, Tyr 139, Thr 184				

Table 5.6 Active site amino acid and hydrogen bond informationfrom docking results of aldehyde pyrazolone, reference ligand and approved drug (Continue…)

Query Molecule	Predicted Target	PDB ID	Respective Acyl Pyrazolone		Reference Ligand		Approved / Experimental Drug	
			No. of H Bonds & its energy (kcal/mol)	Active site Amino acid Residues	No. of H Bonds & its energy (kcal/mol)	Active site Amino acid Residues	No. of H Bonds & its energy (kcal/mol)	Active site Amino acid Residues
APTPMP-3,4F	Class 2 dihydroorotate dehydrogenase, mitochondrial	1D3H	4 (-3.77)	Leu 46, Pro 52, Ala 55, His 56, Ala 59, Val 134, Val 143, Asn 145, Tyr 147, Ser 305, Tyr 356, Thr 357, Thr 360	1 (-2.5)	Met 43, Pro 52, His 56, Ala 59, Thr 63, Phe 98, Met 111, Tyr 356, Leu359, Thr 360, Pro 364	6 (-6.01)	Pro 52, Ala 55, His 56, Arg 136, Val 143, Asn 145, Thr 285, Ser 305, Tyr 356, Thr 357, Thr 360
APTPMP-2,4ME	Class 2 dihydroorotate dehydrogenase, mitochondrial	1D3H	1 (-4.58)	Ala 96, Lys 100, Lys 255, Thr 283, Asn 284, Thr 285, Ser 305, Leu 309, Val 333, Gly 334, Gly 335, , Tyr 356, Thr 357	1 (-2.5)	Met 43, Pro 52, His 56, Ala 59, Thr 63, Phe 98, Met 111, Tyr 356, Leu359, Thr 360, Pro 364	6 (-6.01)	Pro 52, Ala 55, His 56, Arg 136, Val 143, Asn 145, Thr 285, Ser 305, Tyr 356, Thr 357, Thr 360

Table 5.7 Docking results of O-Vanillin, reference ligand, approved drug and inhibitors with their predicted targets

Query Molecule	Predicted Target	PDB ID	Mechanism/ Disease involved	Docking Energy (kcal/mol)					
				Respective O-Vanillin	Reference Ligand	Approved / Experimental Drug		Inhibitors from chEMBL	
						From	To	From	To
V-4BR	Orotidine 5-phosphate decarboxylase	1LP6	Rate limiting step for Methane production	**-90.52**	-96.77	-	-	-	-
	RNA dependent RNA polymerase	1YVX	Hepatitis C Virus	-88.03	-153.16	-123.48	-98.75	-142.01	-87.43
MMM	Prothrombin	3C1K	Prevent Blood coagulation	**-112.23**	-137.53	-167.62	-96.78	-211.89	-112.64
	Androgen receptor	1E3G	Cancer	-93.54	-122.18	-145.23	-98.08	-157.51	-57.73
V-2,4ME	**Prothrombin**	**3C1K**	**Prevent Blood coagulation**	**-138.00**	**-117.53**	**-167.62**	**-96.78**	**-211.89**	**-112.64**

Table 5.8 Active site amino acid and hydrogen bond informationfrom docking results of O-vanillin, reference ligand and approved drug

Query Molecule	Predicted Target	PDB ID	Respective Acyl Pyrazolone		Reference Ligand		Approved / Experimental Drug	
			No. of H Bonds & its energy (kcal/mol)	Active site Amino acid Residues	No. of H Bonds & its energy (kcal/mol)	Active site Amino acid Residues	No. of H Bonds & its energy (kcal/mol)	Active site Amino acid Residues
V-4BR	Orotidine 5-phosphate decarboxylase	1LP6	4 (-7.0)	Lys 72, Leu 123, Met 126, Ser 127, His 128, Gly 156, Pro 157, Ser 158, Pro 180, Ile 200	12 (-13.6)	Lys 72, Leu 123, Met 126, Ser 127, His 128, Val 155, Gly 156, Pro 157, Ser 158	-	-
MMM	Prothrombin	3C1K	4 (-6.57)	Asp 189, Ala 190, Cys 191, Val 213, Trp 215, Gly 216, Gly 219, Gly 226, Phe 227, Tyr 228	6 (-0.23)	His 57, Tyr 60, Leu 99, Ile 174, Asp 189, Ala 190, Cys 191, Glu 192, Ser 195, Val 213, Ser 214, Trp 215, Gly 216, Glu 217, Gly 219, Gly 226	2 (-2.82)	Asp 189, Ala 190, Ser 195, Val 213, Ser 214, Gly 219, Cys 220, Gly 226, Phe 227
V-2,4ME	Prothrombin	3C1K	3 (-5.95)	Leu 99, Asp 189, Ala 190, Glu 192,Ser 195, Val 213, Gly 216, Gly 219, Gly 226, Tyr 228	6 (-0.23)	His 57, Tyr 60, Leu 99, Ile 174, Asp 189, Ala 190, Cys 191, Glu 192, Ser 195, Val 213, Ser 214, Trp 215, Gly 216, Glu 217, Gly 219, Gly 226	2 (-2.82)	Asp 189, Ala 190, Ser 195, Val 213, Ser 214, Gly 219, Cys 220, Gly 226, Phe 227

Figure 5.3: Docking result ofacyl pyrazolonePTPMP-EA, Reference Ligand and Approved drug with Caspase-1(PDB ID: 1BMQ). Color Scheme of PyMOL image: Green-PTPMP-EA, Red-Reference Ligand, and Cyan-Approved Drug.

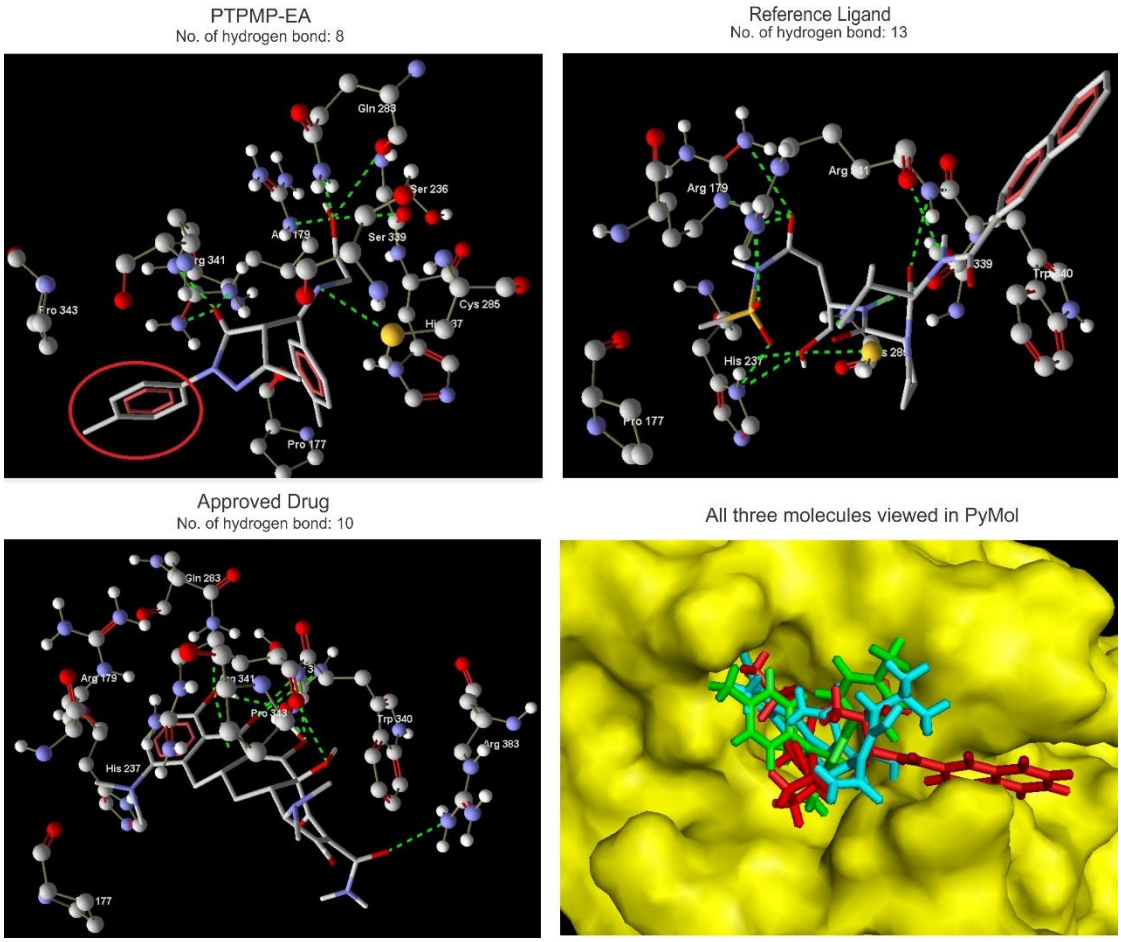

Though the software predicted acyl pyrazolone PMP-EA to bind with Gag-Pol polyprotein (Protease) of HIV (PDB ID: 1HXW) the docking score failed to produce better affinity than approved drugs. Genome polyprotein (RNA Polymerase) (PDB ID: 1YVX) of Hepatitis C Virus shows better docking score (-120.22 kcal/mol) than experimental drug 3-[(2,4-Dichlorobenzoyl)(Isopropyl)Amino]-5-Phenylthiophene-2-Carboxylic Acid (DrugBank ID: DB03388) (-98.75 kcal/mol). The reference ligand 3-[Isopropyl(4-Methylbenzoyl)Amino]-5-Phenylthiophene- 2-Carboxylic acid provided lowest docking energy (-153.16 kcal/mol) than any other molecules [445]. The active site amino acid residues Thr 418, Ile 419, Arg 422, Met 423, Thr 476, Tyr 477, Lys 501 and Trp 528 are responsible for the binding of PMP-EA with 7 hydrogen bonds and hydrogen bond energy (Binding energy) -6.0 kcal/mol which is better binding

energy than other molecules. The RMSD of PMP-EA and approved drug is 3.8 Å. Hence, the PMP-EA has higher binding affinity with the target.

Figure 5.4A: Docking result ofacyl pyrazolonePMP-EA, Reference Ligand and Approved drug with Genome polyprotein (RNA polymerase) (PDBID: 1YVX). Color Scheme of PyMOL image: Green-PMP-EA, Red-Reference Ligand, and Cyan-Approved Drug.

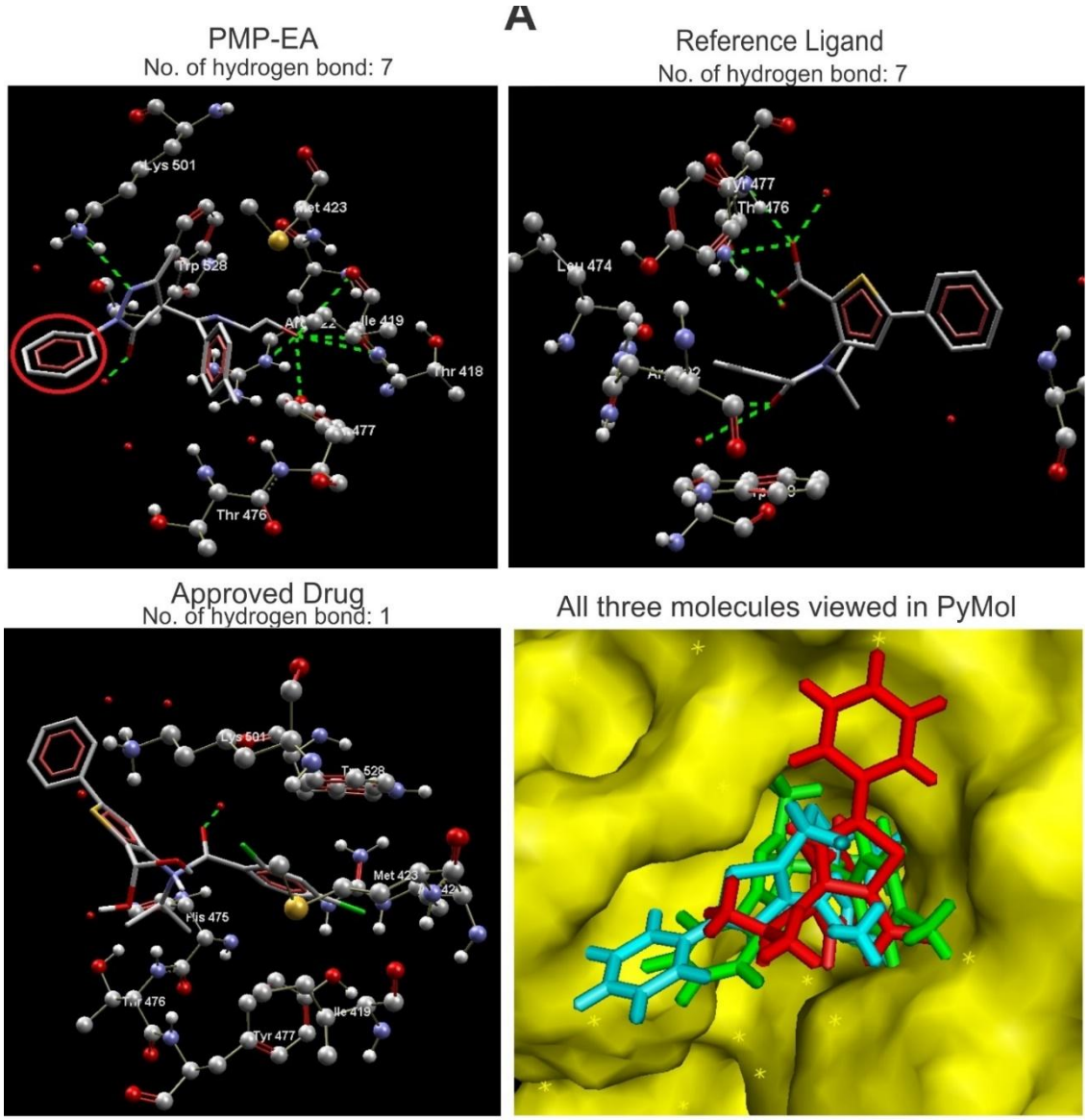

PMP-EA binds with another protein Tyrosine-protein phosphatase non-receptor type 1 (PDB ID: 1Q6N) with best docking score (-153.58 kcal/mol) than the available approved drug Tiludronate (DrugBank ID: DB01133) (-90.42 kcal/mol). Although the co-crystal molecule {4-[(2s,4e)-2-(1,3-Benzothiazol-2-Yl)-2-(1h-1,2,3-Benzotriazol-1-Yl)-5-Phenylpent-4-Enyl]Phenyl}(Difluoro)Methylphosphonic Acid

[417] provides best docking score (-255.40 kcal/mol) with 17 hydrogen bonds and -12.7 kcal/mol binding energy compared with all molecules, it fails to be a drug. The active site amino acid residues Ala 517, Gln 521, Arg 1047, Asp 1048, Val 1049, Phe 1182, Ala 1217, Gly 1220, Arg 1221 and Gln 1262 are responsible for the binding of PMP-EA with 3 hydrogen bonds and hydrogen bond energy (Binding energy) -2.5 kcal/mol which is not better binding energy than other molecules though it provides better docking score due to other internal forces.

Figure 5.4B: Docking result ofacyl pyrazolonePMP-EA, Reference Ligand and Approved drug withTyrosine-protein phosphatase non-receptor type 1(PDB ID: 1Q6N). Color Scheme of PyMOL image: Green-PMP-EA, Red-Reference Ligand, and Cyan-Approved Drug.

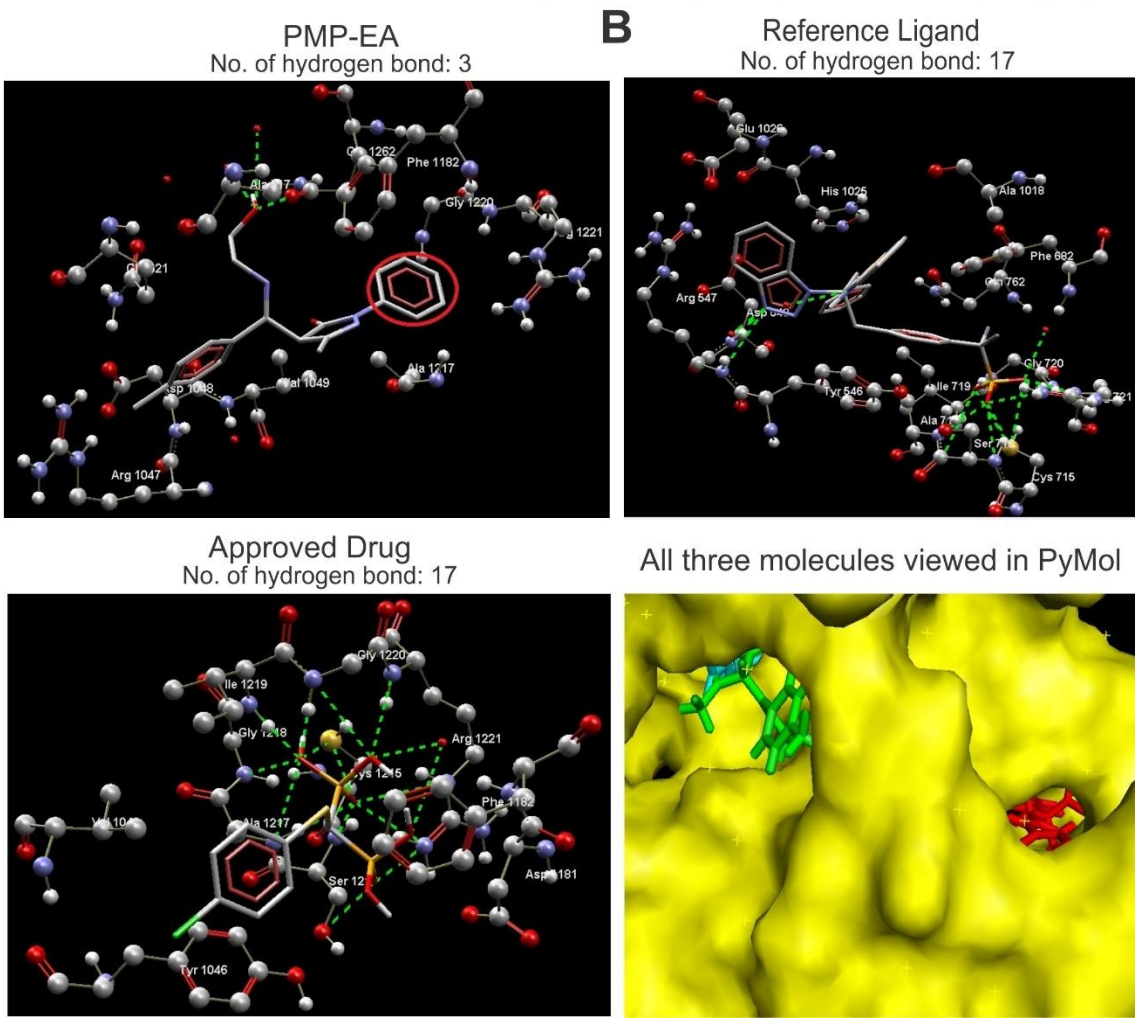

Although the approved drug possesses 17 hydrogen bonds with binding energy -12.7 kcal/mol, it fails to generate better docking score. Interestingly, the approved drug and the PMP-EA binds together with the same pocket of target protein with 3.8 Å distance and co-crystal inhibitor binds with another pocket of the target protein.

Figure 5.5: Docking result ofacyl pyrazoloneMCPMP-EA, Reference Ligand and Approved drug with Estrogen sulfotransferase (PDB ID: 1G3M). Color Scheme of PyMOL image: Green-MCPMP-EA, Red-Reference Ligand, and Cyan-Approved Drug.

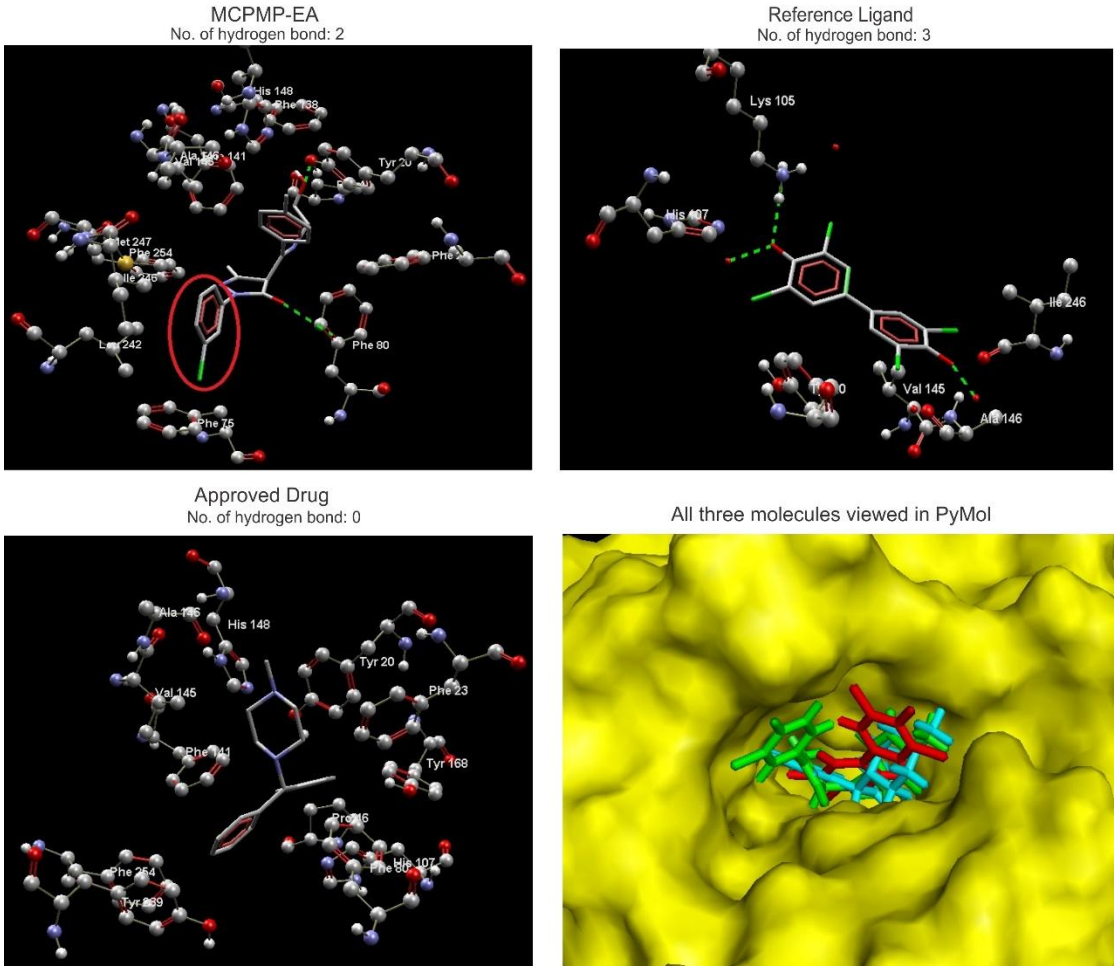

The acyl pyrazolone MCPMP-EA binds with Estrogen sulfotransferase (PDB ID: 1G3M) with docking score -131.72 kcal/mol, 2 hydrogen bonds with binding energy -2.5 kcal/mol which is better than approved drug Cyclizine (DrugBank ID: DB01176).

Figure 5.6: Docking result ofaldehyde pyrazoloneAPTPMP-4BR, Reference Ligand and Approved drug with mitochondrial Class 2 dihydroorotate dehydrogenase (PDB ID: 1D3H). Color Scheme of PyMOL image: Green-APTPMP-4BR, Red-Reference Ligand, and Cyan-Approved Drug.

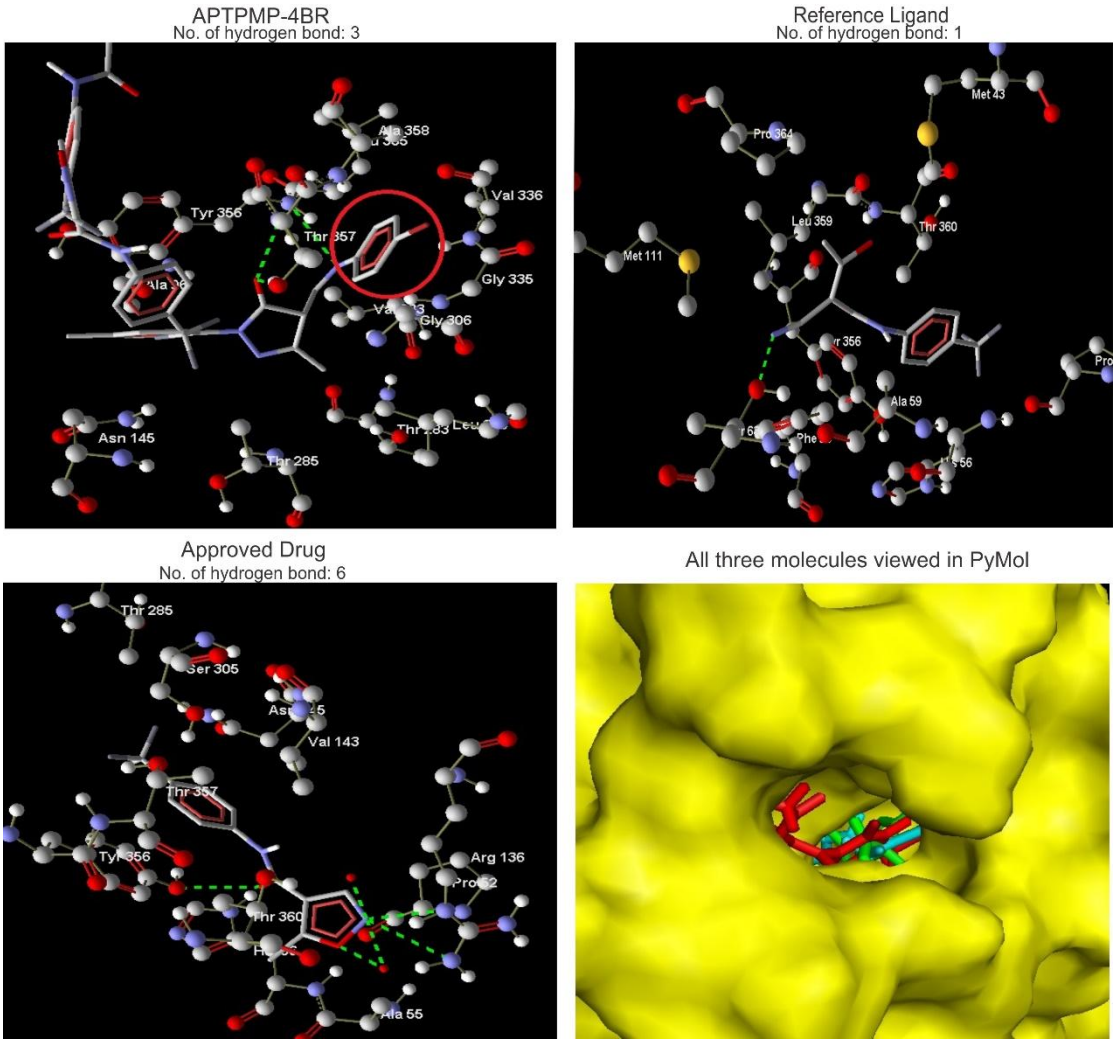

The active site amino acid residues Tyr 20, Phe 23, Pro 46, Phe 75, Phe 80, Phe 138, Phe 141, Val 145, Ala 146, His 148, Leu 242, Ile 246, Met 247 and Phe 254 are responsible for the binding of PMP-EA with the pocket of protein target. Although the MCPMP-EA, co-crystal inhibitor and approved drug binds with same pocket, the MCPMP-EA and approved drug are away from each other by 4.7 Å distance. The co-crystal inhibitor 3,5,3',5'-Tetrachloro-Biphenyl-4,4'-Diol [446] binds with target with undesirable docking score (-95.96 kcal/mol).

The aldehyde pyrazoloneAPTPMP-4BR, APTPMP-4F, APTPMP-3,4F and APTPMP-2,4ME binds with mitochondrial Class 2 dihydroorotate dehydrogenase (DHODH, class 2) (PDB ID: 1D3H). APTPMP-4BR binds with docking score of -136.64 kcal/mol which is better than the docking score (-127.36 kcal/mol) of approved drug but, the hydrogen bond interactions of approved drug Leflunomide (DrugBank ID: DB01097) provides 6 hydrogen bonds with lower binding energy (-6.01 kcal/mol) than APTPMP-4BR which has 3 hydrogen bonds with binding energy -2.5 kcal/mol. The co-crystal molecule (2Z)-2-cyano-3-hydroxy-N-[4-(trifluoromethyl)phenyl]but- 2-enamide [425]shows higher docking score (-113.64 Kcal / mol) than approved drug and APTPMP-4BR with only one hydrogen bond with same binding energy (-2.5 kcal/mol) of approved drug. The approved drug and APTPMP-4BR binds in the same pocket of protein but, each is 2.194 Åaway from the other.

Figure 5.7: Docking result ofaldehyde pyrazoloneAPTPMP-4F, Reference Ligand and Approved drug with mitochondrial Class 2 dihydroorotate dehydrogenase (PDB ID: 1D3H). Color Scheme of PyMOL image: Green-APTPMP-4F, Red-Reference Ligand, and Cyan-Approved Drug.

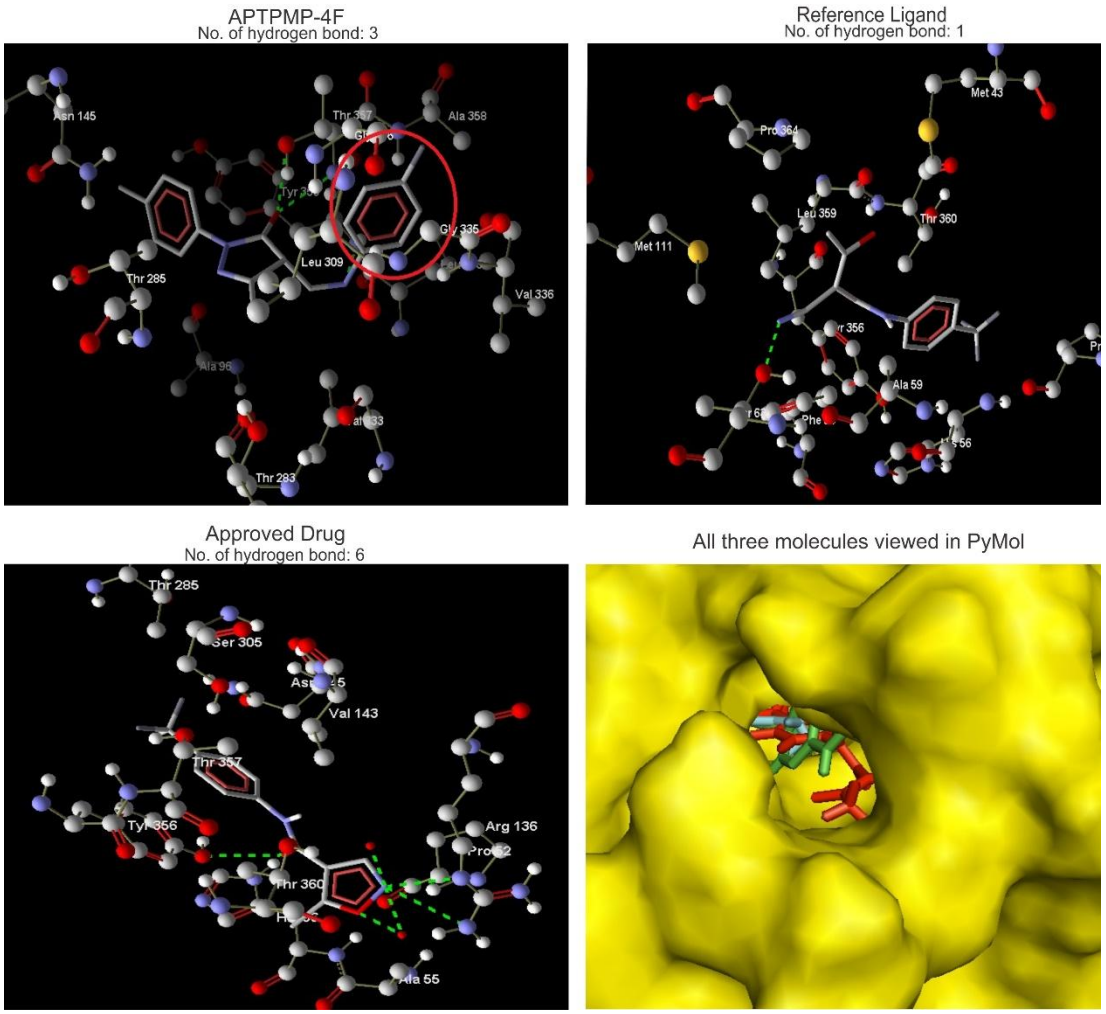

The active site amino acids Ala 96, Asn 145, Thr 283, Thr 285, Gly 306, Leu 309, Val 333, Gly 335, Val 336, Leu 355, Tyr 356, Thr 357 and Ala 358 are responsible for the binding of APTPMP-4BR.

The aldehyde pyrazolone APTPMP-4F provides better docking score (-143.85 kcal/mol) than approved drug but, only 3 hydrogen bonds with binding energy -4.56 kcal/mol which is poor than approved drug. Both molecules are away from each other by 2.762 Å distance. The same 13 amino acids residues responsible for binding of APTPMP-4BR are also responsible to bind APTPMP-4F with the pocket of protein.

Figure 5.8: Docking result ofaldehyde pyrazoloneAPTPMP-4F, Reference Ligand and Approved drug with Heat shock protein HSP 90-alpha (PDB ID: 1UY6). Color Scheme of PyMOL image: Green-APTPMP-4F, Red-Reference Ligand, and Cyan-Approved Drug.

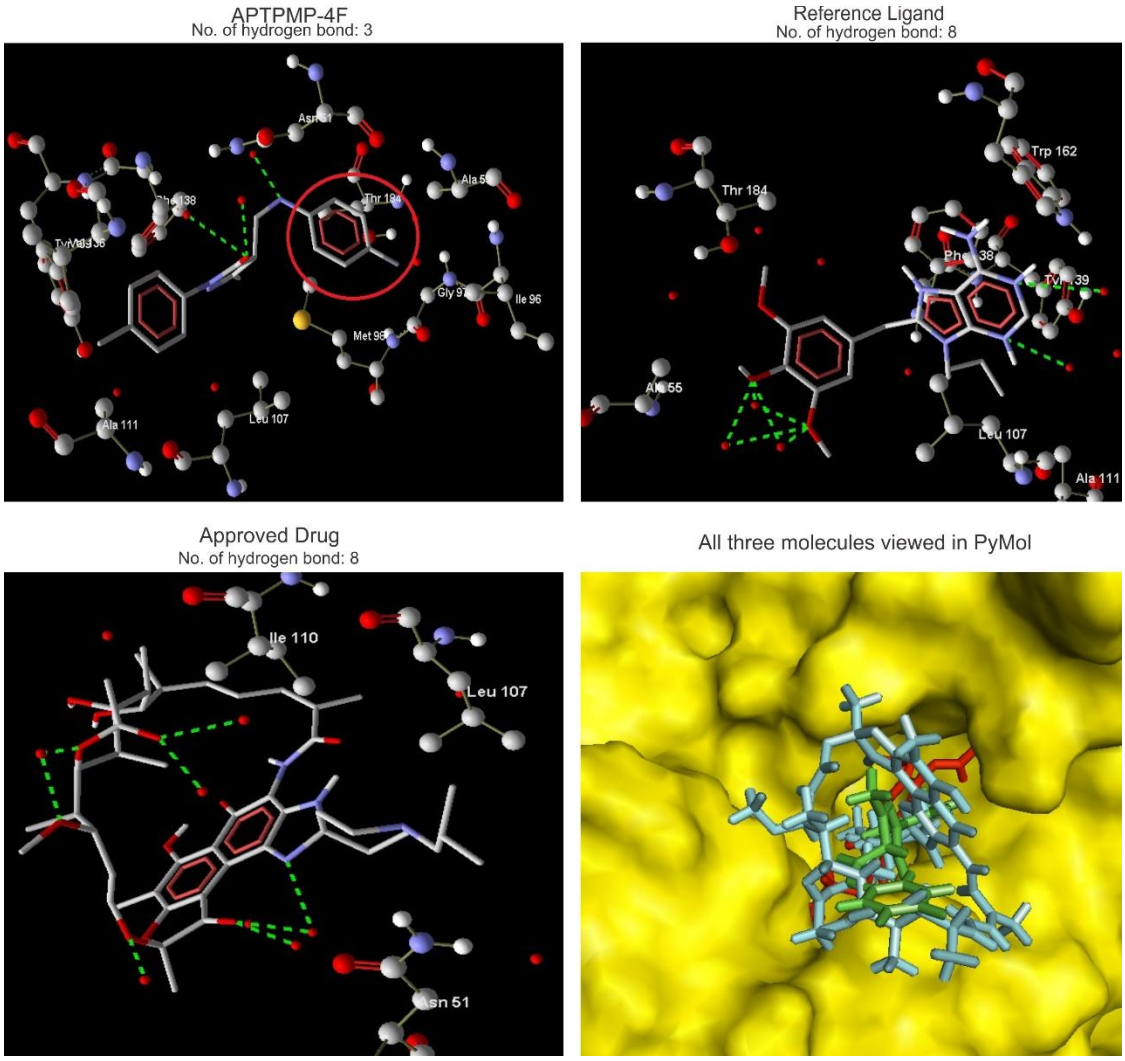

APTPMP-3,4F provides better docking score (-136.68 kcal/mol) than approved drug but, only 4 hydrogen bonds with binding energy -3.77 kcal/mol which is poorer than approved drug. Both molecules are away from each other by 4.800 Å which is a high distance. The active site amino acids Leu 46, Pro 52, Ala 55, His 56, Ala 59, Val 134, Val 143, Asn 145, Tyr 147, Ser 305, Tyr 356, Thr 357 and Thr 360 are responsible for the binding of APTPMP-3,4F.

Figure 5.9: Docking result ofaldehyde pyrazoloneAPTPMP-3,4F, Reference Ligand and Approved drug with mitochondrial Class 2 dihydroorotate dehydrogenase (PDB ID: 1D3H). Color Scheme of PyMOL image: Green- APTPMP-3,4F, Red-Reference Ligand, and Cyan-Approved Drug.

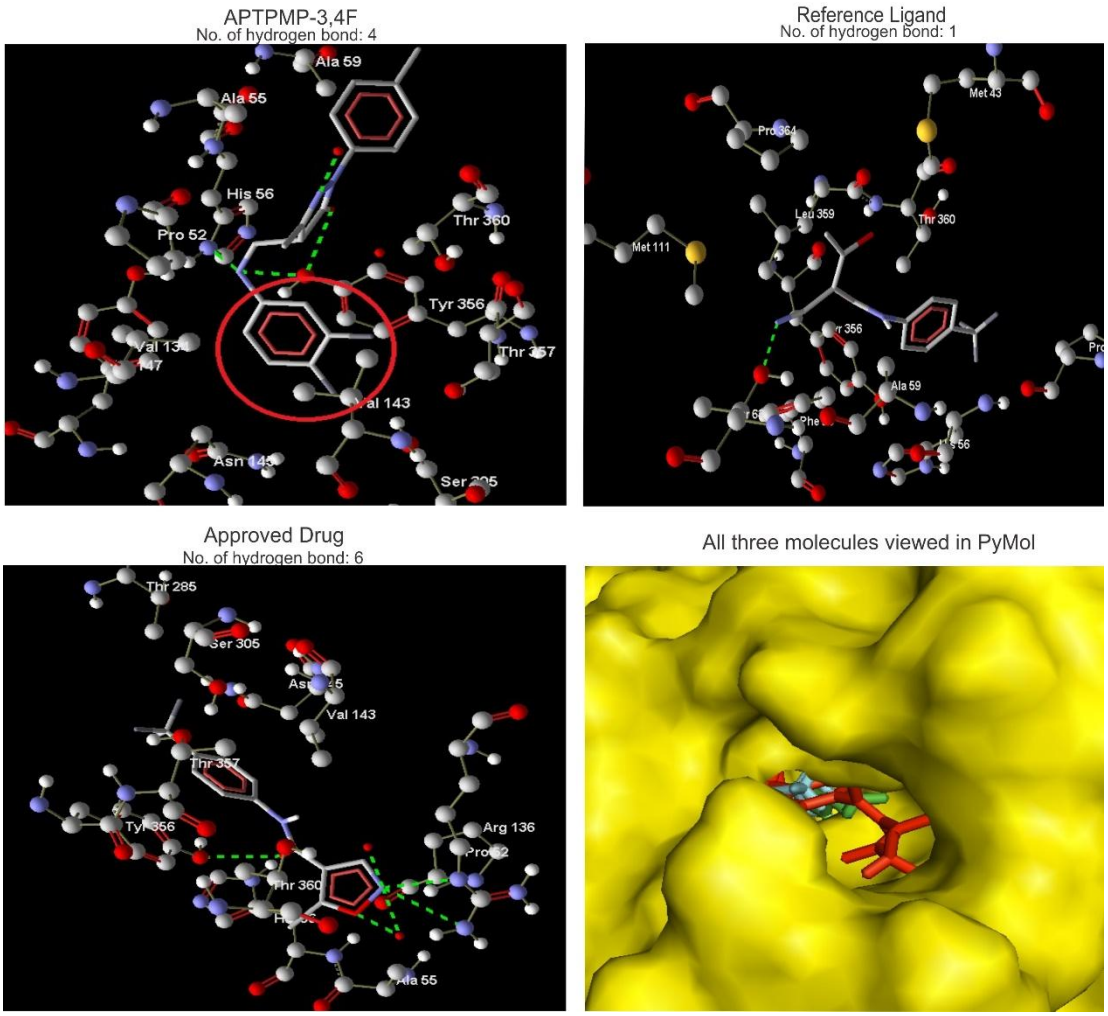

APTPMP-2,4ME provides better docking score (-144.99 kcal/mol) than approved drug but, has only one hydrogen bond with binding energy -4.58 kcal/molwhich is better than approved drug. APTPMP-2,4ME and the approved drug are binding with protein with a distance of 2.293 Å. The active site amino acids residues Ala 96, Lys 100, Lys 255, Thr 283, Asn 284, Thr 285, Ser 305, Leu 309, Val 333, Gly 334, Gly 335, Tyr 356 and Thr 357 are responsible for the binding of APTPMP-3,4F[447].

Figure 5.10: Docking result ofaldehyde pyrazoloneAPTPMP-2,4ME, Reference Ligand and Approved drug with mitochondrial Class 2 dihydroorotate dehydrogenase (PDB ID: 1D3H). Color Scheme of PyMOL image: Green-APTPMP-2,4ME, Red-Reference Ligand, and Cyan-Approved Drug.

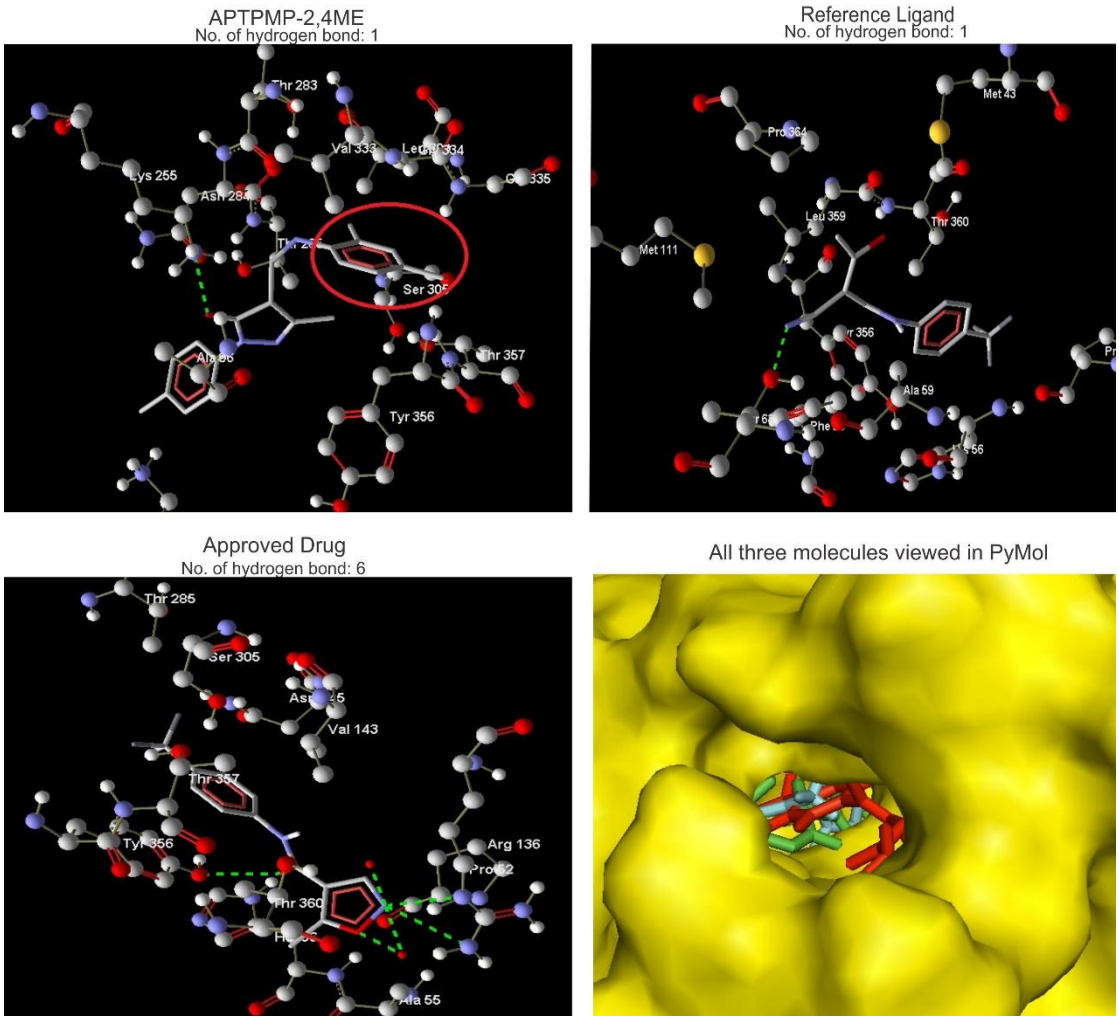

The aldehyde pyrazolone APTPMP-4F also responsible to bind with Heat shock protein HSP 90-alpha (PDB ID: 1UY6) with better docking score (-113.43 kcal/mol) than the approved drug Rifabutin (DrugBank ID: DB00615) (-58.73 kcal/mol). Significantly the APTPMP-4F, approved drug and the co-crystal (reference ligand) ligand 9-Butyl-8-(3,4,5-Trimethoxybenzyl)-9h-purin- 6-amine are bonded with the protein [448] with zero hydrogen bond energy. The APTPMP-4F has 3 hydrogen bonds compared to 8 hydrogen bonds in approved drug and reference ligand. The active site amino acids areAsn 51, Ala 55, Ile 96, Gly 97, Met 98, Leu 107, Ala 111, Val 136, Phe 138, Tyr 139 andThr 184. The APTPMP-4F and approved drugs bind with the protein pocket with 3.790 Å distance between each other.

The O-vanillin V-4BR binds with Orotidine 5-phosphate decarboxylase (PDB ID: 1LP6) with docking score -90.52 kcal/mol, which is higher energy than the reference (Co-crystal) ligand (-96.77 kcal/mol) Cytidine-5'-monophosphate [437]. Total 12 hydrogen bonds with binding energy -13.6 kcal/mol is involved in the

binding of reference ligand with protein but, only 4 hydrogen bonds with -7.0 Kcal energy is involved in the binding of V-4BR with the protein. The amino acids responsible for the binding of V-4BR are Lys 72, Leu 123, Met 126, Ser 127, His 128, Gly 156, Pro 157, Ser 158, Pro 180 and Ile 200. The reference ligand and the V-4BR bind with the protein with 3.424 Å distance between the two.

Figure 5.11: Docking result ofO-VanillinV-4BR and Reference Ligand with Orotidine 5-phosphate decarboxylase (PDB ID: 1LP6). Color Scheme of PyMOL image: Green-V-4BR and Red-Reference Ligand.

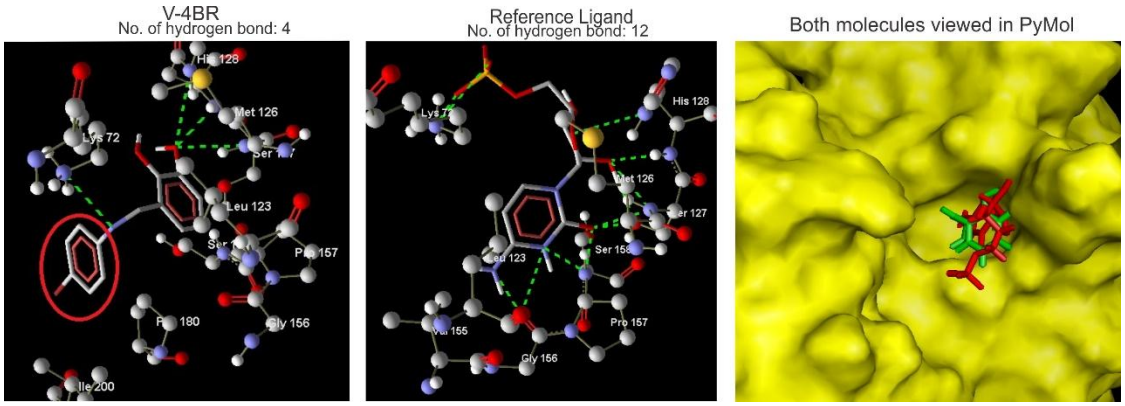

The O-Vanillin derivatives MMM and V-2,4ME binds with Prothrombin (PDB ID: 3C1K). MMM binds with better docking score (-112.23kcal/mol) than the approved drug Menadione (DrugBank ID: DB00170) (-96.78 kcal/mol). Significantly, the nitrogen in the modified group is involved in the hydrogen bond formation. The MMM has 4 hydrogen bonds with binding energy -6.57 kcal/mol which is better than the approved drug having 2 hydrogen bond with binding energy -2.82 kcal/mol. The active site amino acids Asp 189, Ala 190, Cys 191, Val 213, Trp 215, Gly 216, Gly 219, Gly 226, Phe 227 and Tyr 228 are responsible to bind MMM with a protein. The MMM and approved drugs bind with the protein pocket with 3.248 Å distance between each other.

Figure 5.12: Docking result ofO-VanillinMMM, Reference Ligand and Approved drug with Prothrombin (PDB ID: 3C1K). Color Scheme of PyMOL image: Green-MMM, Red-Reference Ligand, and Cyan-Approved Drug.

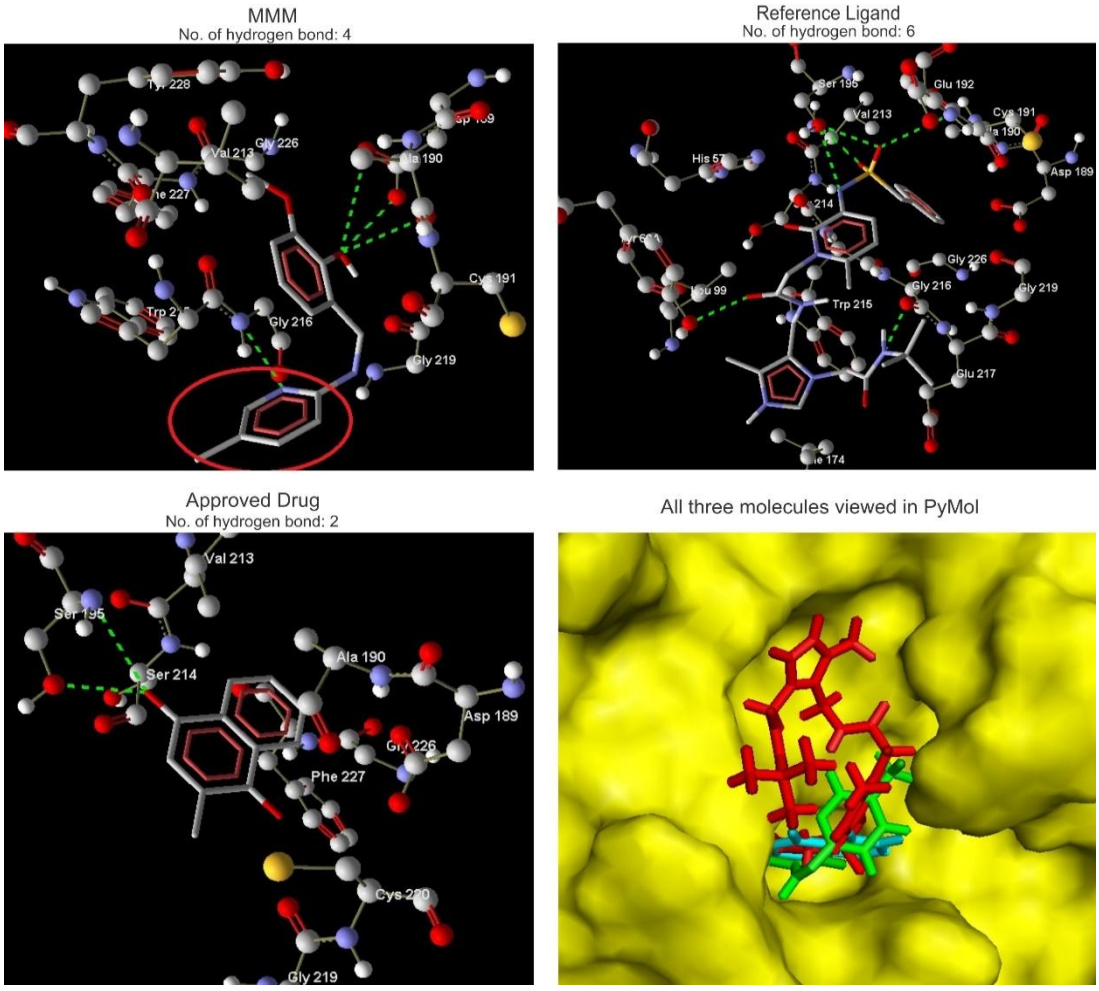

The O-vanillin derivative V-2,4ME binds with better docking score (-138.00 kcal/mol) than the approved drug Menadione (DrugBank ID: DB00170) (-96.78 kcal/mol) and the reference ligand2-{3-[(benzylsulfonyl)amino]-6-methyl-2-oxopyridin- 1(2H)-yl}-N-({1-[2-(tert-butylamino)-2-oxoethyl]-4-methyl-1H-imidazol-5-yl}methyl)acetamide(-117.53kcal/mol). The 4-VF has 3 hydrogen bonds with binding energy -5.95 kcal/mol which is better than the approved drug having 2 hydrogen bond with binding energy -2.82 kcal/mol. The active site amino acids His 57, Asp 189, Ala 190, Cys 191, Val 213, Gly 216, Gly 219, Gly 226 and Tyr 228 are responsible to bind 4-VF with a protein. The 4-VF and approved drugs bind in the protein pocket with 3.227 Å distance between the two. Although the reference ligand 2-{3-[(benzylsulfonyl)amino]-6-methyl-2-oxopyridin- 1(2H)-yl}-N-({1-[2-(tert-butylamino)-2-oxoethyl]- 4-methyl-1H-imidazol-5-yl}methyl)acetamide[439]and the collected inhibitors from chEMBL provide better docking score than the MMM and V-2,4ME, they failed in the drug likeliness property.

Figure 5.13: Docking result ofO-VanillinV-2,4ME, Reference Ligand and Approved drug with Prothrombin (PDB ID: 3C1K). Color Scheme of PyMOL image: Green-V-2,4ME, Red-Reference Ligand, and Cyan-Approved Drug.

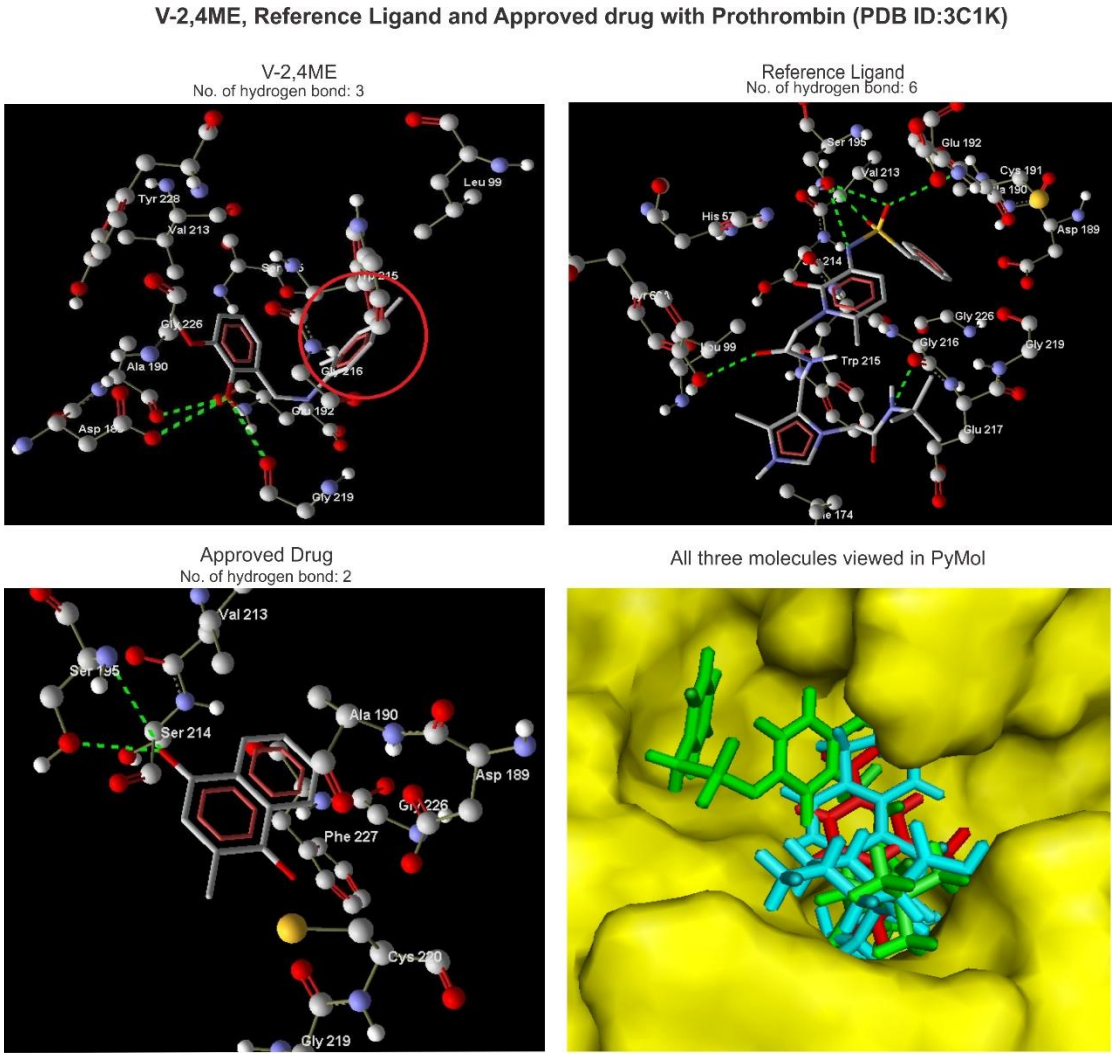

5.3.4 Molecular dynamics simulation studies

As a case study, the best docked score protein-ligand complex from each one of acyl and aldehyde pyrazolone and o-vanillin was performed to observe the stability of the complex by molecular dynamics simulation study.

The acyl pyrazolone MCPMP-EA bound with Estrogen sulfotransferase (PDB ID: 1G3M) was considered for molecular dynamics study as it had the docking score -131.72 kcal/mol and 2 hydrogen bonds with binding energy -2.5 kcal/molwhich was

better than the approved drug Cyclizine (DrugBank ID: DB01176) (docking score -92.10 kcal/mol) and the Reference Ligand (docking score -95.96 kcal/mol).

To analyse the stability and overall conformational changes of acyl pyrazolone MCPMP-EA with Estrogensulfotransferase (PDB ID: 1G3M), the Root mean square deviation (RMSD), Root mean square fluctuations (RMSF) and the Protein-ligandcontacts were studied.

Figure 5.14: Root mean square deviation (RMSD) of acyl pyrazolone MCPMP-EA with Estrogen sulfotransferase (PDB ID: 1G3M)

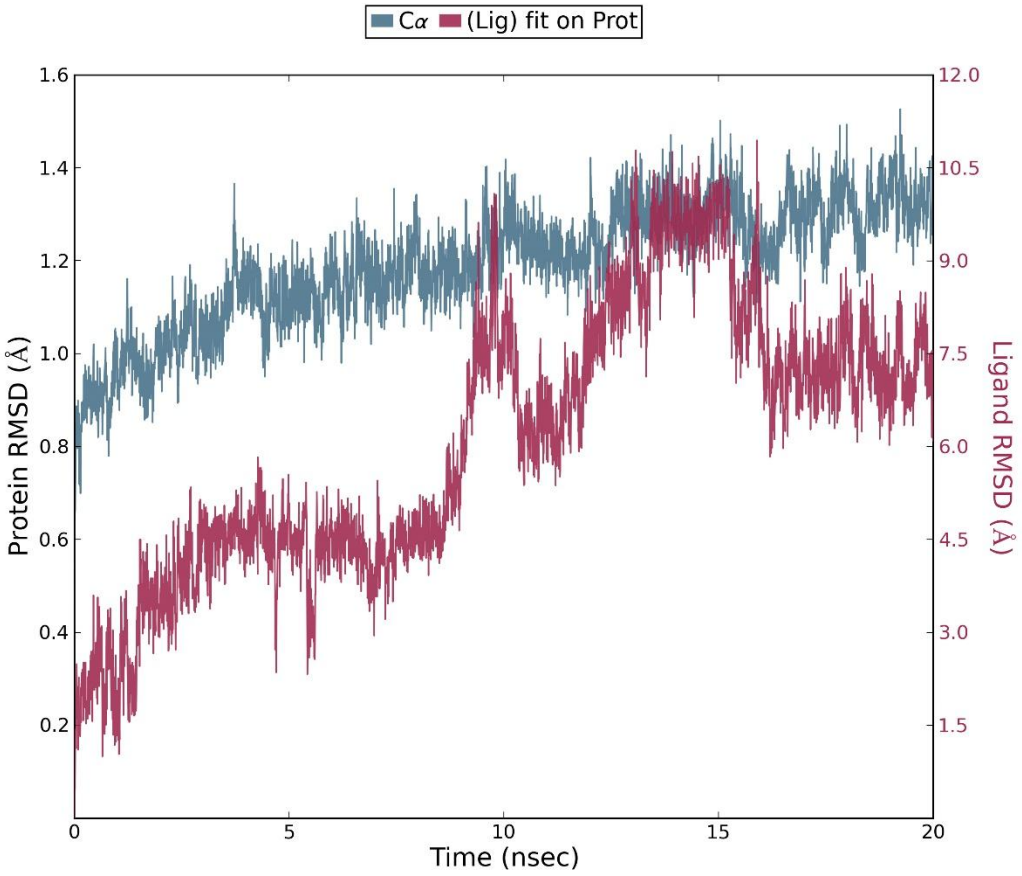

Figure 5.15a: Root mean square fluctuations (RMSF) of Estrogen sulfotransferase (PDB ID: 1G3M)

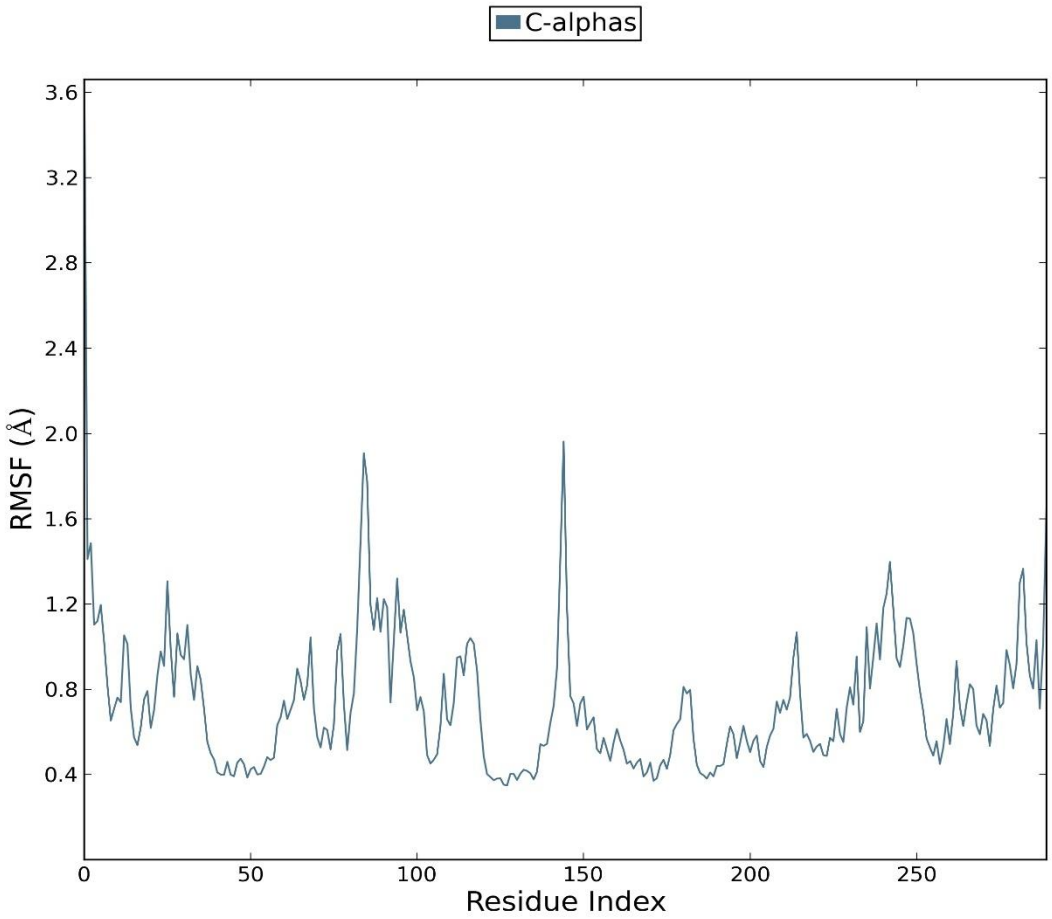

In order to understand the conformational changes in the protein-ligand complex, RMSD of the protein's c-alpha chain, backbone, side chains and heavy atoms present in the protein wasanalyzed along with the RMSD of ligand with reference to the docked ligand conformation. When the RMSD of the protein Estrogen sulfotransferase was analyzed, the RMSD was steadily increasing from 0.8 A^0 at 1 ns time to 1.3 A^0 at 20 ns time (Figure 5.14). It was nearly within the acceptable range of 1-3 Å [409]. Changes much larger than 1-3 Åindicate that the protein is undergoing a large conformational change during the simulation. But in case of ligand, RMSD varies from 1.5 A^0 at 1 ns to 10.5 A^0 at 20 ns time and it varies highly between 9 ns and 16 ns, then becomes stable till 20 ns (Figure 5.14). As the ligand RMSD values observed are significantly larger at later stagethan that of the RMSD of the protein, it is inferred that ligandis likely to diffuse away from its initial binding site.

The Root Mean Square Fluctuation (RMSF) is useful for characterizing local changes along the protein chain and the ligand atom positions. The amino acid

residues are flexible in the range between 0.4 A^0 and 2.0 A^0. Only two amino acids show high flexibility (Figure 5.15a). The ligand is comparatively stable (2.5-3.2 A^0) from the atom number 1 to 22 and flexible from atom number 23 to 26 (2.5-5.0 A^0) which has -N–CH_2-CH_2-OH group (Figure 5.15b). Significantly, this –OH group makes a hydrogen bond with Phe 80 of active site residues which is also flexible.

Figure 5.15b: Root mean square fluctuations (RMSF) of acyl pyrazolone MCPMP-EA

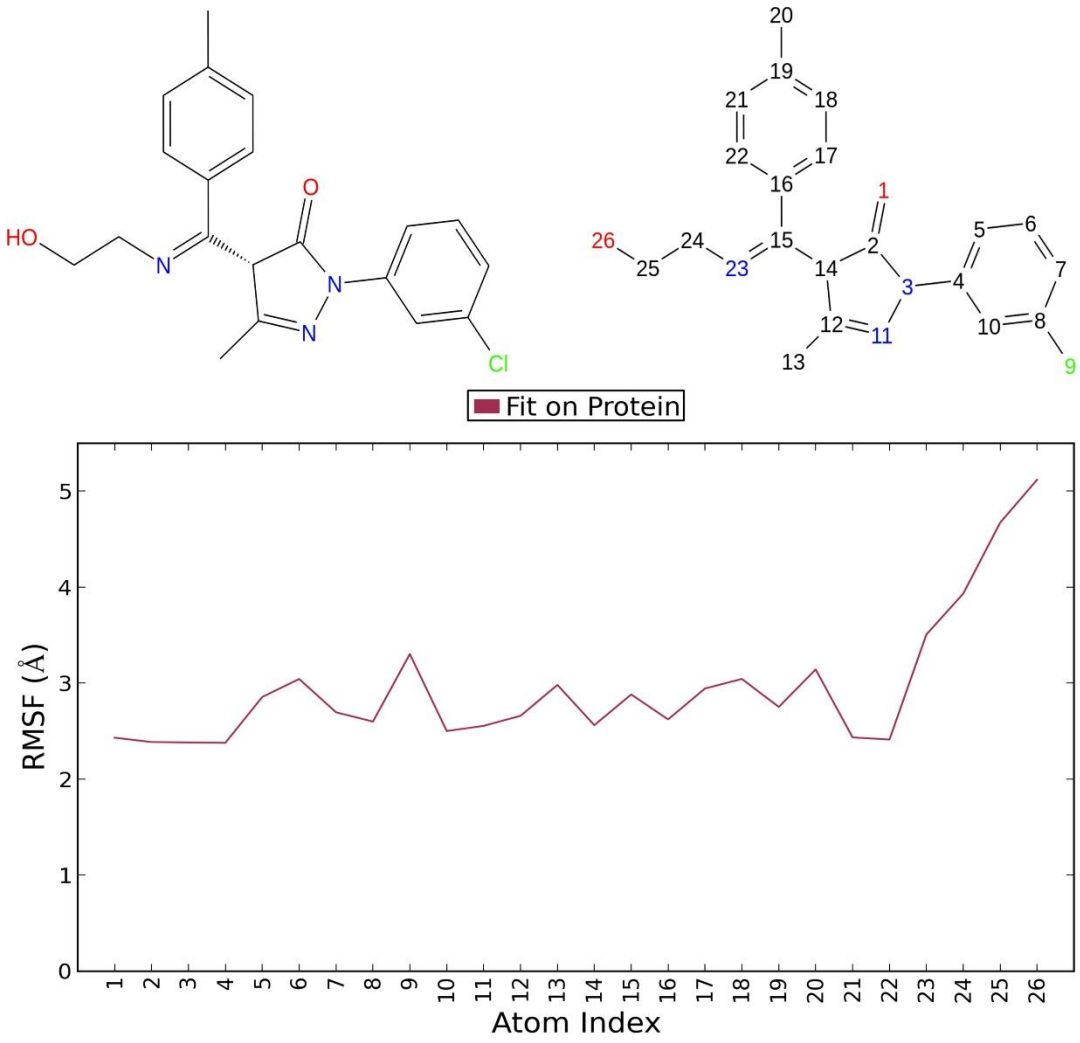

Protein interactions with the ligand was monitored throughout the simulation. These interactions are categorized by type and summarized in the figure 5.16. Protein-ligand interactions (or 'contacts') are categorized into four types: Hydrogen Bonds, Hydrophobic, Ionic and Water Bridges. The stacked bar charts are normalized over the course of the trajectory: for example, a value of 0.7 suggests that 70% of the simulation time the specific interaction is maintained. Among four types of bonds,

hydrogen bonds (H-bonds) play a significant role in ligand binding. Consideration of hydrogen-bonding properties in drug design is important because of their strong influence on drug specificity, metabolization and adsorption. Hydrogen bonds between a protein and a ligand can be further broken down into four subtypes: backbone acceptor; backbonedonor; side-chain acceptor; side-chain donor. The current geometric criteria for protein-ligand H-bond is: distance of 2.5 Å between the donor and acceptor atoms (D—H···A); a donor angle of ≥120° between the donor-hydrogen-acceptor atoms (D—H···A); and an acceptor angle of ≥90° between the hydrogen-acceptor-bonded atoms (H···A—X).

Figure 5.16: Interactions of Estrogen sulfotransferase (PDB ID: 1G3M) with acyl pyrazolone MCPMP-EA

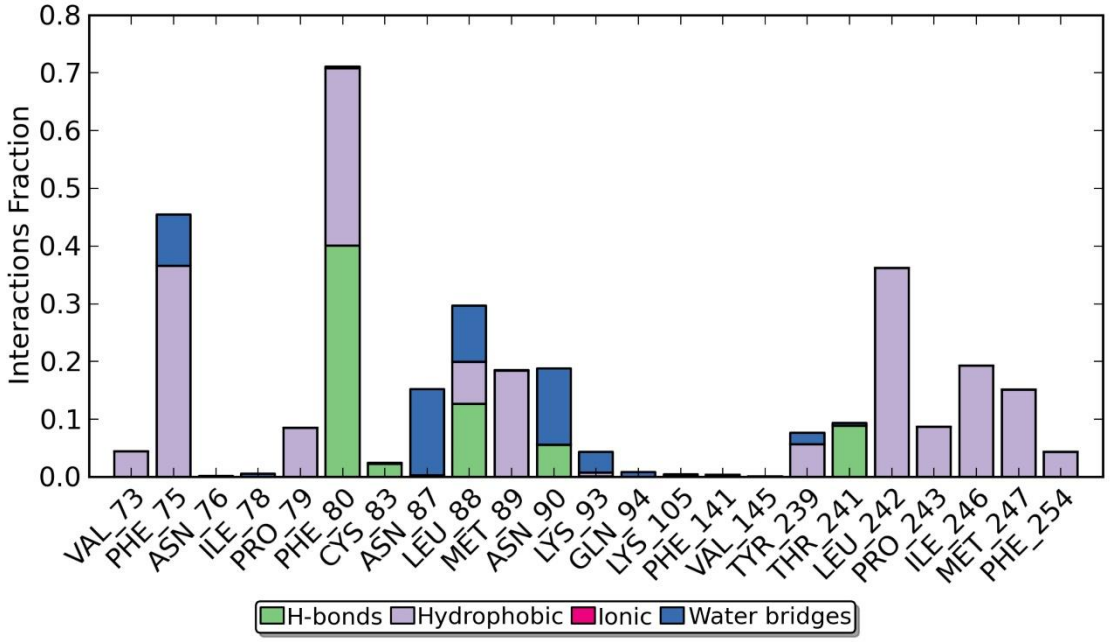

A timeline representation of the interactions and contacts (H-bonds, Hydrophobic, Ionic, Water bridges)summarized in figure 5.17. The top panel shows the total number of specific contacts that the proteinmakes with the ligand over the course of the trajectory. The bottom panel shows which residues interact withthe ligand in each trajectory frame. Some residues make more than one specific contact with the ligand,which is represented by a darker shade of orange, according to the scale to the right of the plot. The amino acid Phe 80 makes a good hydrogen bond interaction during the first 10 ns;later, it is not making good hydrogen bond interaction with ligand. The amino acids Phe 75 and Leu 242 discontinuously contact

the ligand and other active site amino acids shown in the figure have different interacting patterns throughout the simulation time. A schematic of detailed ligand atom interactions with the protein residues is shown in figure 5.18. The interactions that occur more than 30.0% of the simulation time in the selected trajectory (0.00 through 20.00 ns) are shown. It is possible to have interactions with >100% as some residues may have multiple interactions of asingle type with the same ligand atom. For example, the ARG side chain has four H-bond donors that can allhydrogen-bond to a single H-bond acceptor. Figure 5.18 shows that the amino acid Phe 80 and Leu 242 havea hydrogen bond with more than 40% of simulation time and hydrophobic interaction respectively.

Figure 5.17: A timeline representation of the interactions and contacts (H-bonds, Hydrophobic, Ionic, Water bridges) between MCPMP-EA and Estrogen sulfotransferase (PDB ID: 1G3M)

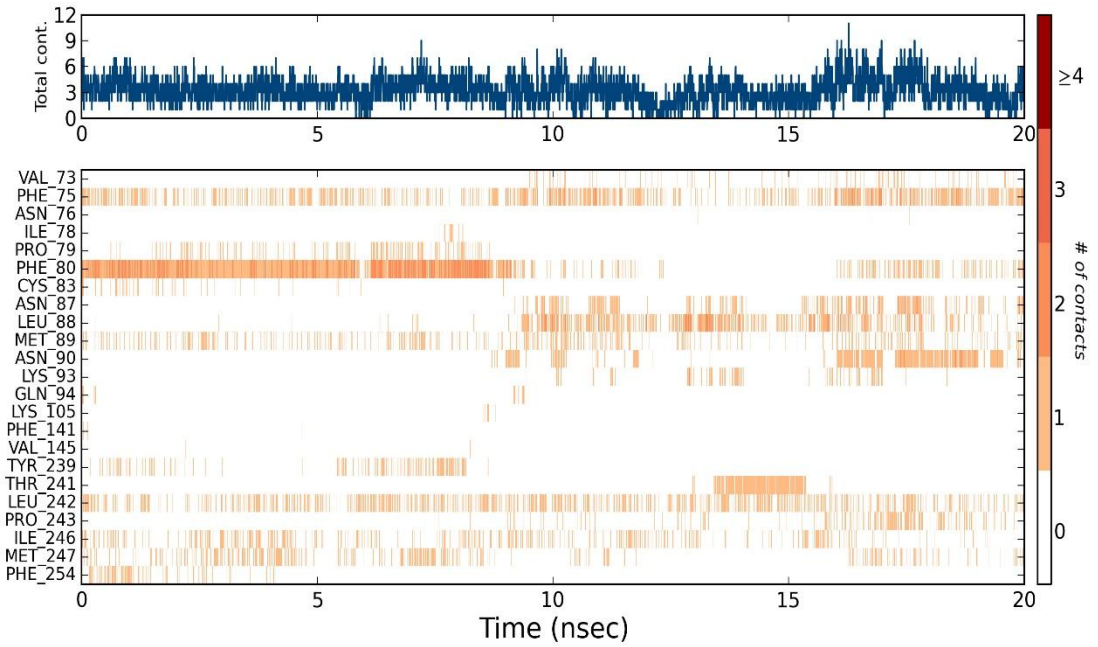

The aldehyde pyrazolone APTPMP-2,4ME bound with mitochondrial class 2 dihydroorotate dehydrogenase (PDB ID: 1D3H) was considered for molecular dynamic study as it had the docking score -144.99 kcal/mol andone hydrogen bonds with binding energy -4.58 kcal/mol which was better docking score than approved drug: Leflunomide (DrugBank ID: DB01097) (-127.36 kcal/mol) and the Reference Ligand: (2Z)-2-cyano-3-hydroxy-N-[4-(trifluoromethyl)phenyl]but- 2-enamide (docking score -113.64 kcal/mol).

Figure 5.18: A schematic of detailed MCPMP-EA atom interactions with the Estrogen sulfotransferase amino acid residues.

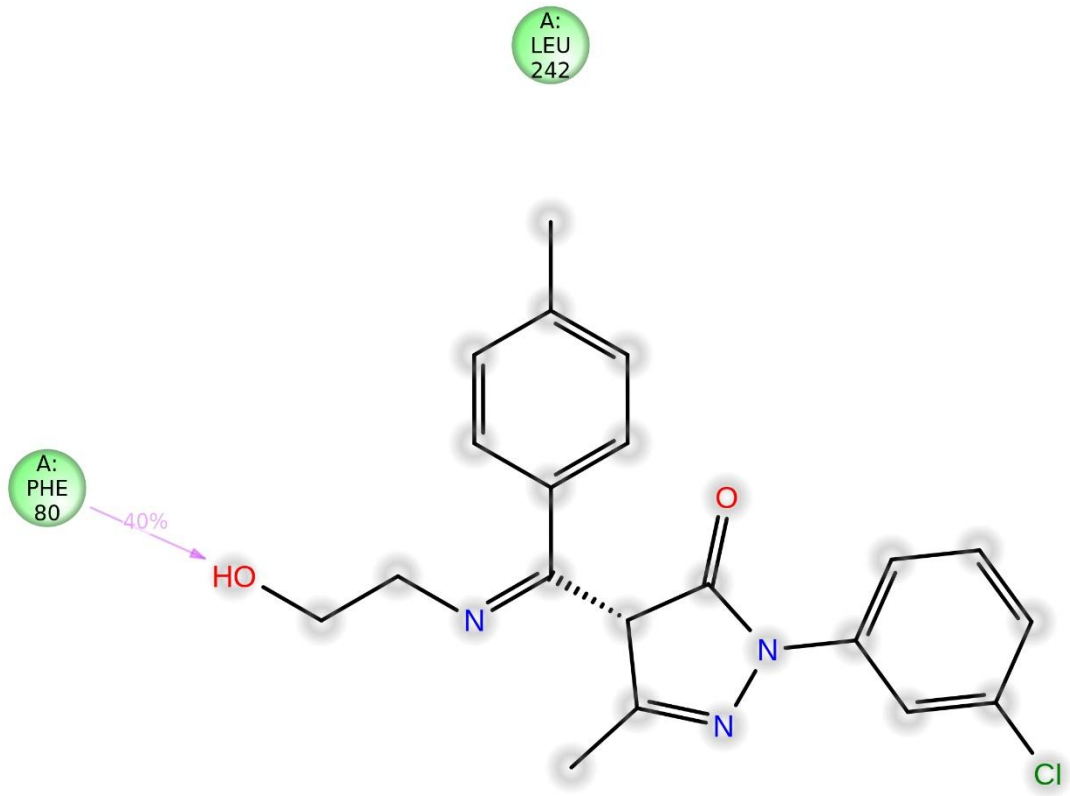

To analyse the stability and overall conformational changes of aldehyde pyrazolone APTPMP-2,4ME with Estrogen sulfotransferase (PDB ID: 1D3H) the Root mean square deviation (RMSD), Root mean square fluctuations (RMSF) and the Protein-ligand contacts were studied.

In order to understand the conformational changes in the protein-ligand complex, RMSD of the protein's c-alpha chain, backbone, side chains and heavy atoms present in the protein has been analyzed along with the RMSD of ligand with reference to the docked ligand conformation. The RMSD of the protein,mitochondrial class 2 dihydroorotate dehydrogenase was steady throughout the simulation process except 10 to 14 ns, in which little higher flexibility was observed. But, the overall RMSD value of protein is ranging between 0.8 $A^0$and 4.7A^0 (Figure 5.19). It is little beyond the acceptable range of 1-3 Å [409]. Changes much larger than 1-3 Å indicate that the protein is undergoing a large conformational change during the simulation.

But in case ofa ligand, RMSD varies from 0.2 $A^0$to 1.4 A^0 and varies highly between 0 ns and 10 ns, then stable till 20 ns (Figure 5.19). As the values observed are significantly larger at later duration than the RMSD of the protein, it shows the ligand is likely to diffuse away from its initial binding site.

Figure 5.19: Root mean square deviation (RMSD) of aldehyde pyrazolone APTPMP-2,4ME with mitochondrial class 2 dihydroorotate dehydrogenase (PDB ID: 1D3H)

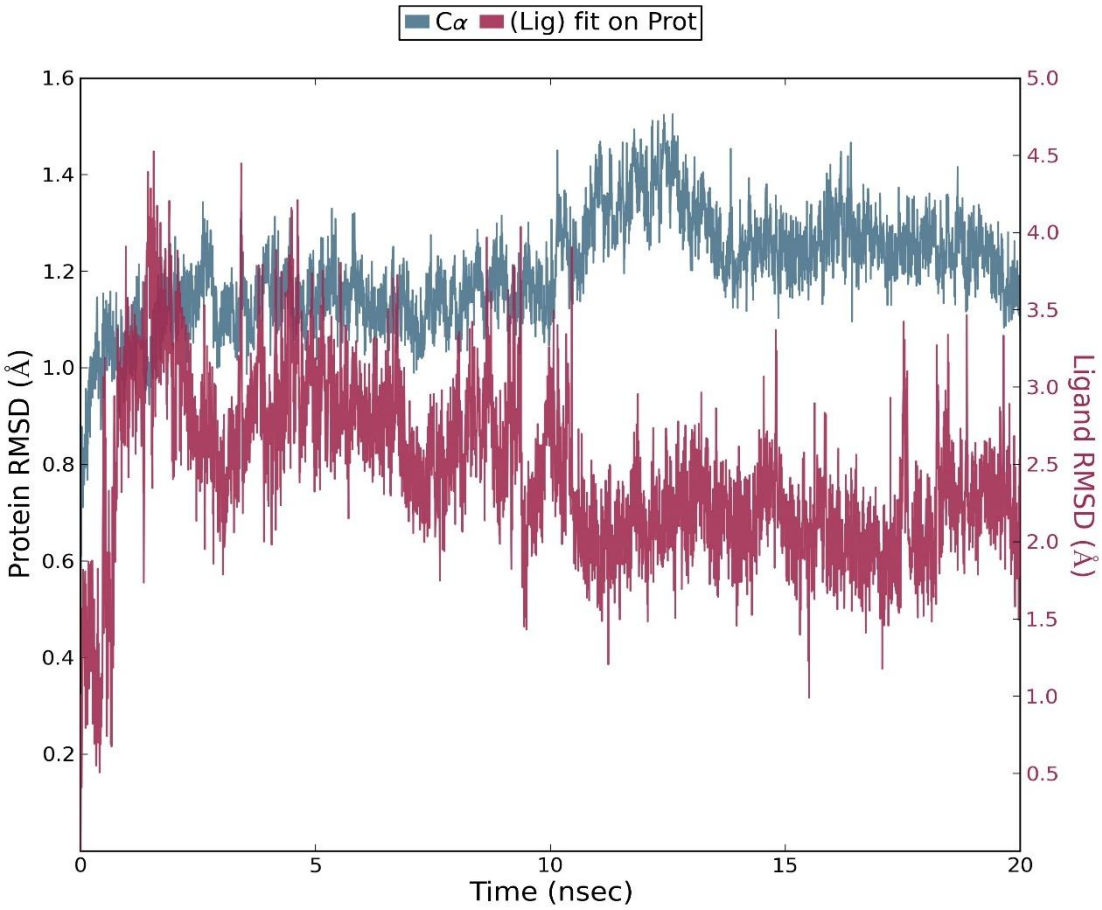

The Root Mean Square Fluctuation (RMSF) is useful for characterizing local changes along the protein chain and the ligand atom positions. Only five amino acids show high flexibility (Figure 5.20a) with the maximum value of 1.6 A^0. Throughout the process, the ligand APTPMP-2,4ME shows the flexibility in the range between0.9 A^0 and 1.4 A^0(Figure 5.20b).

Protein interactions with the ligand were monitored throughout the simulation. Most of the active site amino acids had hydrophobic interaction than the Hydrogen Bonds, Ionic and Water Bridges (Figure 5.21).

Figure 5.20a: Root mean square fluctuations (RMSF) of mitochondrial class 2 dihydroorotate dehydrogenase (PDB ID: 1D3H)

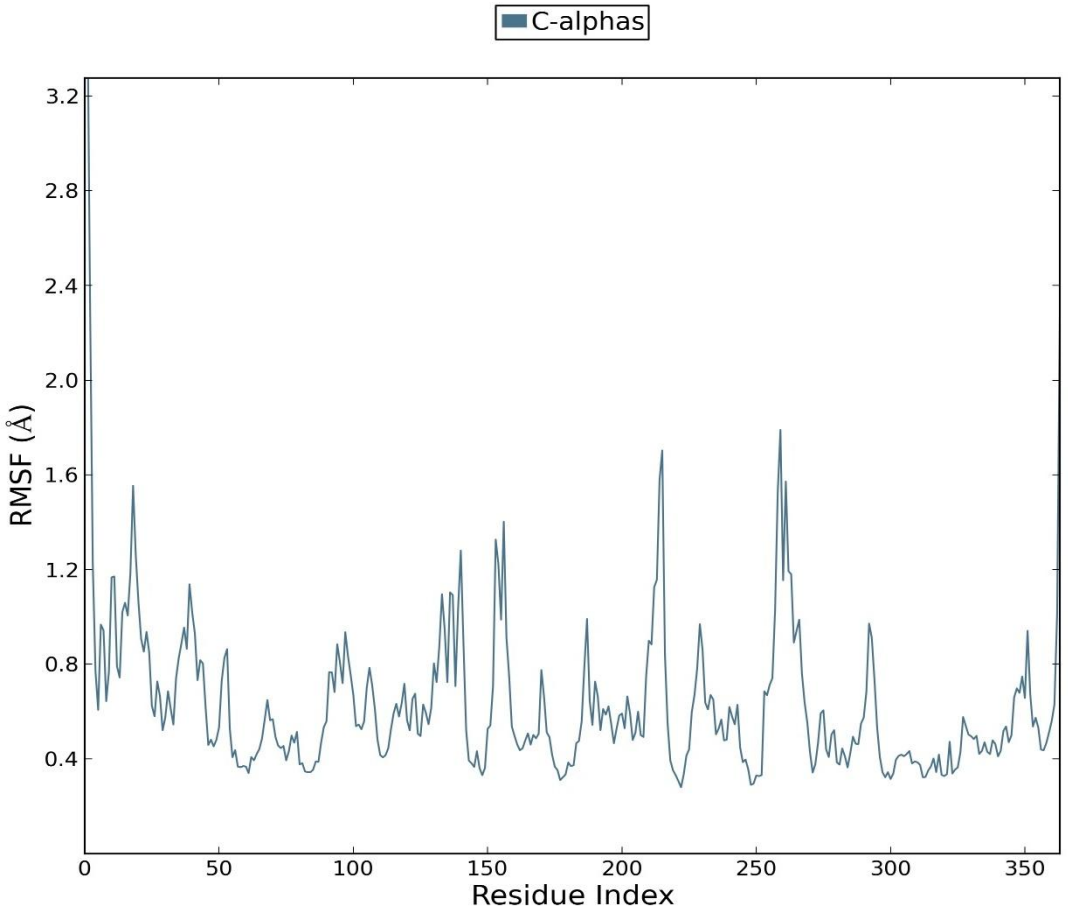

A timeline representation of the protein-ligand interactions and contacts summarized in figure 5.22. The top panel shows the total number of specific contacts the protein makes with the ligand over the course of the trajectory. The bottom panel shows which residues interact with the ligand in each trajectory frame. Some residues make more than one specific contact with the ligand, which is represented by a darker shade of orange, according to the scale to the right of the plot. The active site amino acidshave interaction with ligand maximum of 3.6 ns (18% of 20 ns). Most of them discontinuously contactthe ligand. A schematic of detailed ligand atom interactions with the protein residues is shown in figure 5.23. The interactions that occur more than 10.0% of the simulation time in the selected trajectory (0.00 through 20.00 ns), are shown. The oxygen of ligand molecule contact (Hydrophobic interaction) the amino acid Arg 136 and Thr 360through the intermediate water molecules.

Figure 5.20b: Root mean square fluctuations (RMSF) of aldehyde pyrazolone APTPMP-2,4ME

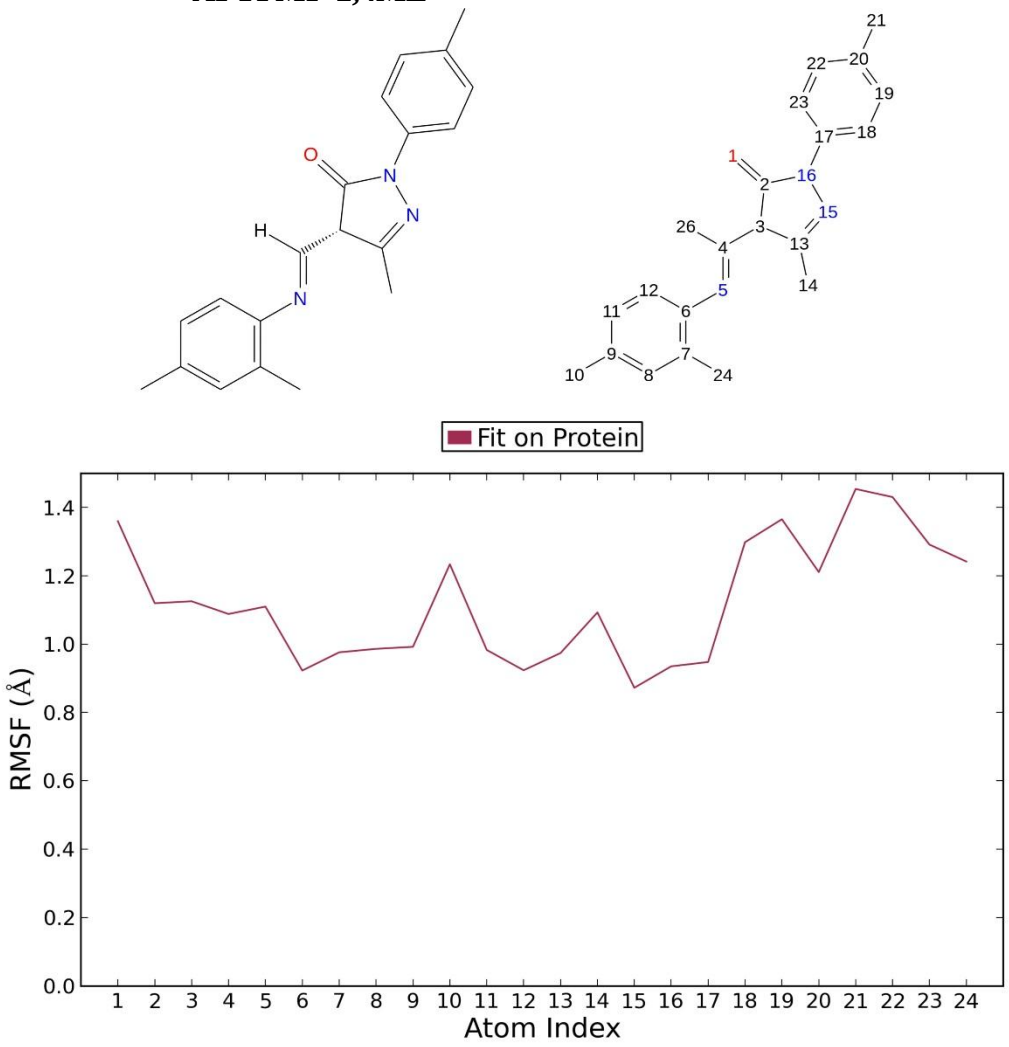

Figure 5.21: Interactions of mitochondrial class 2 dihydroorotate dehydrogenase (PDB ID: 1D3H) with acyl pyrazolone MCPMP-EA

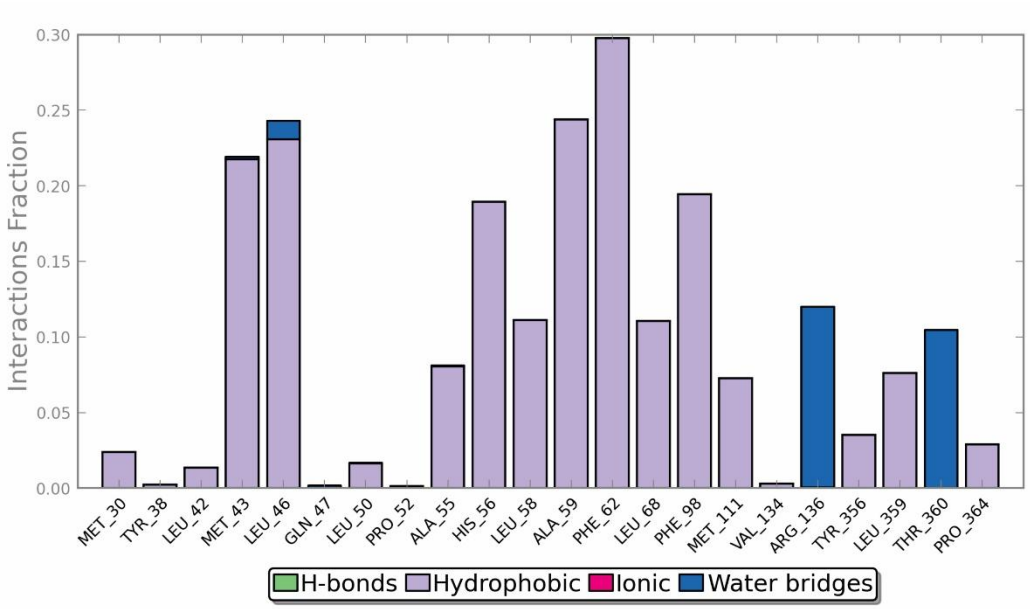

Figure 5.22: A timeline representation of the interactions and contacts (H-bonds, Hydrophobic, Ionic, Water bridges) between APTPMP-2,4ME and mitochondrial class 2 dihydroorotate dehydrogenase

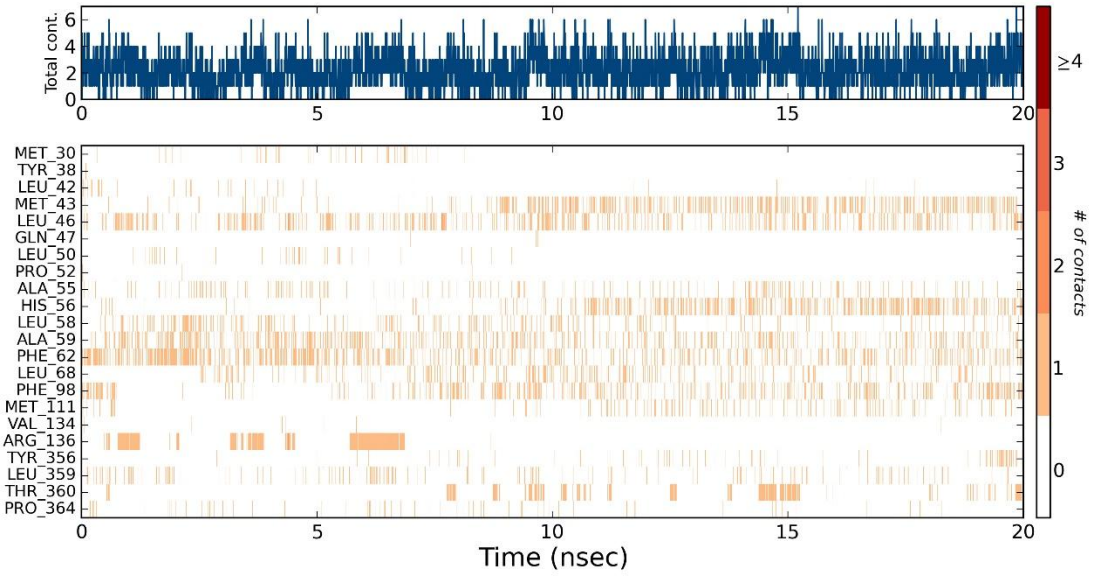

Figure 5.23: A schematic of detailed APTPMP-2,4MEatom interactions with the mitochondrial class 2 dihydroorotate dehydrogenase amino acid residues.

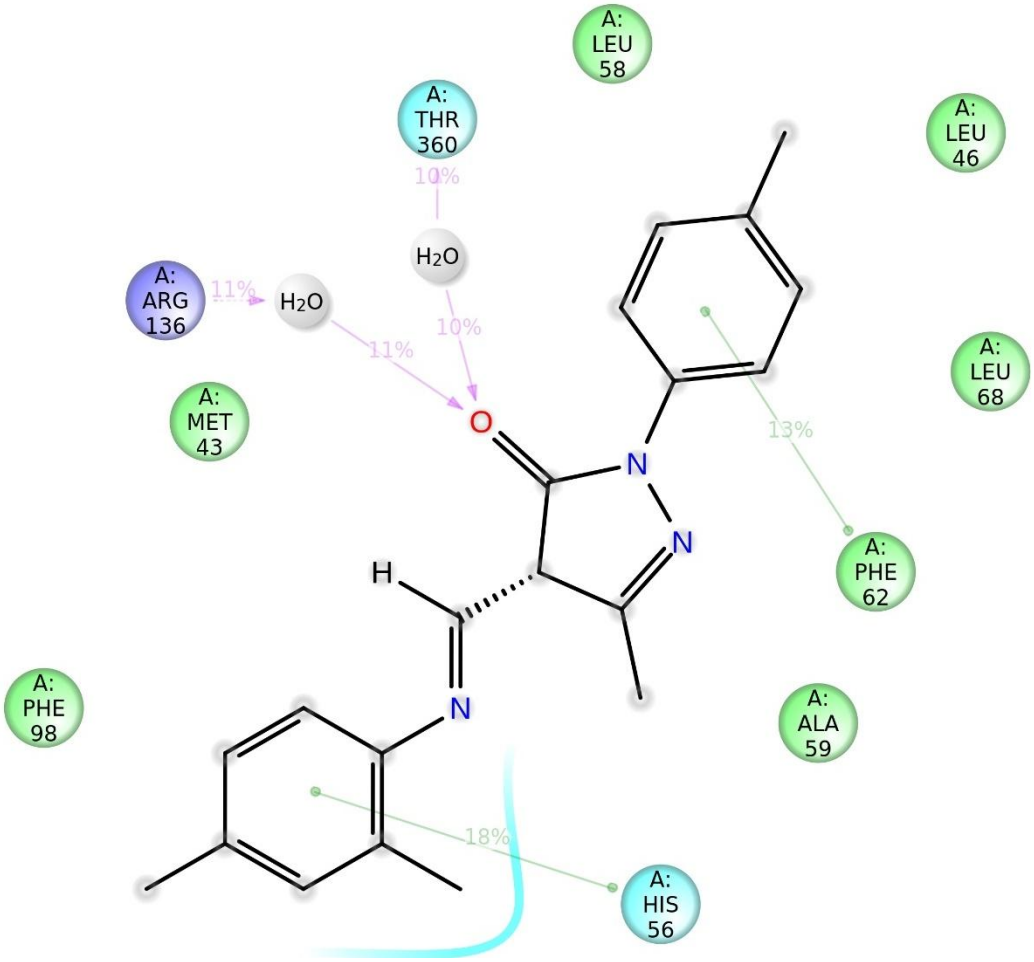

The o-vanillinV-2,4MEbound with Prothrombin (PDB ID: 3C1K) was considered for molecular dynamic study as it had the docking score -138 kcal/mol andthree hydrogen bonds with binding energy -5.95 kcal/mol which is better docking score than approved drug:Menadione (DrugBank ID: DB00170) (-96.78 kcal/mol) and the Reference Ligand:2-{3-[(benzylsulfonyl)amino]-6-methyl-2-oxopyridin-1(2H)-yl}-N-({1-[2-(tert-butylamino)-2-oxoethyl]- 4-methyl-1H-imidazol-5-yl}methyl)acetamide (docking score -117.53 kcal/mol).

Figure 5.24: Root mean square deviation (RMSD) of o-vanillin V-2,4ME with Prothrombin (PDB ID: 3C1K)

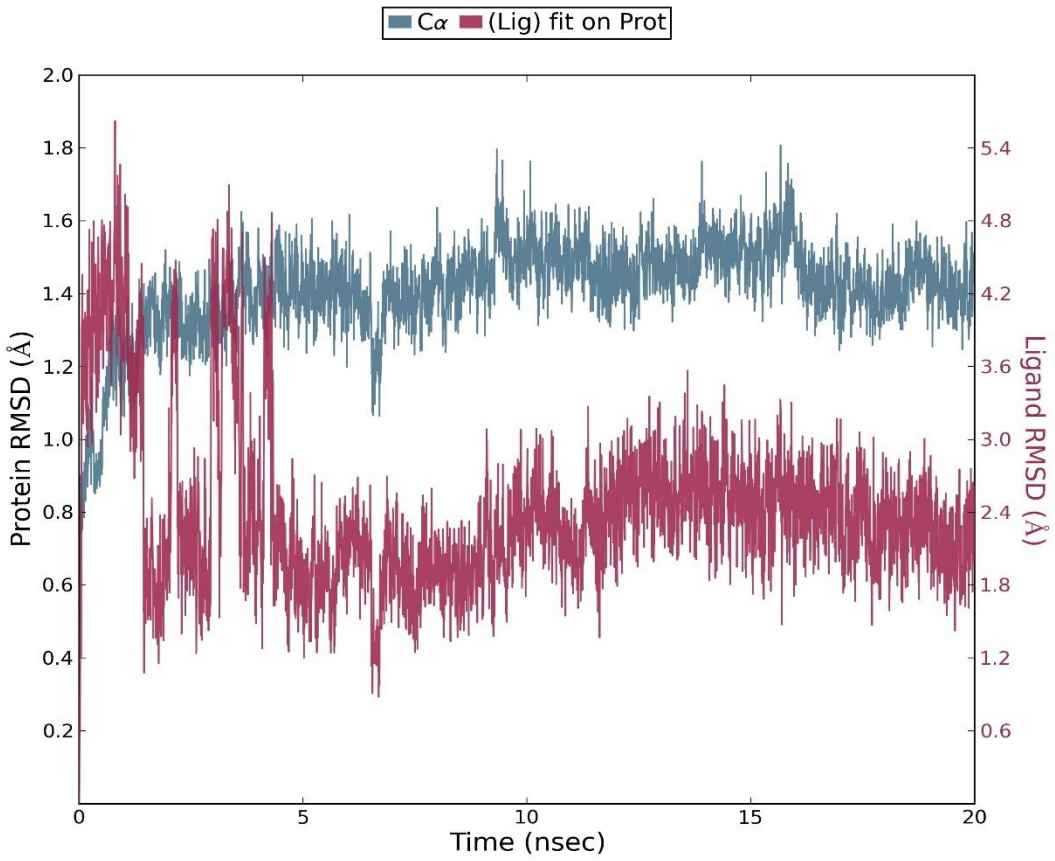

To analyse the stability and overall conformational changes of o-vanillin V-2,4MEwith Prothrombin (PDB ID: 3C1K),the Root mean square deviation (RMSD), Root mean square fluctuations (RMSF) and the Protein-ligand contacts were studied.

The RMSD of Prothrombin was steady throughout the simulation process except 10 to 14 ns, in which little higher flexibility was observed. But, the overall RMSD value of protein is ranging between 0.8 A^0 and 1.7A^0 (Figure 5.24). As the values are within the acceptable range of 1-3 Å [409], the protein doesn't undergo much conformational changes. But the ligand is highly flexible RMSD till 4 ns andlater stage it shows the stability(Figure 5.24). As the values observed are significantly similar to the RMSD of the protein at later stage, it shows the ligand is not likely to diffuse away from its binding site.

Figure 5.25a: Root mean square fluctuations (RMSF) of Prothrombin (PDB ID: 3C1K)

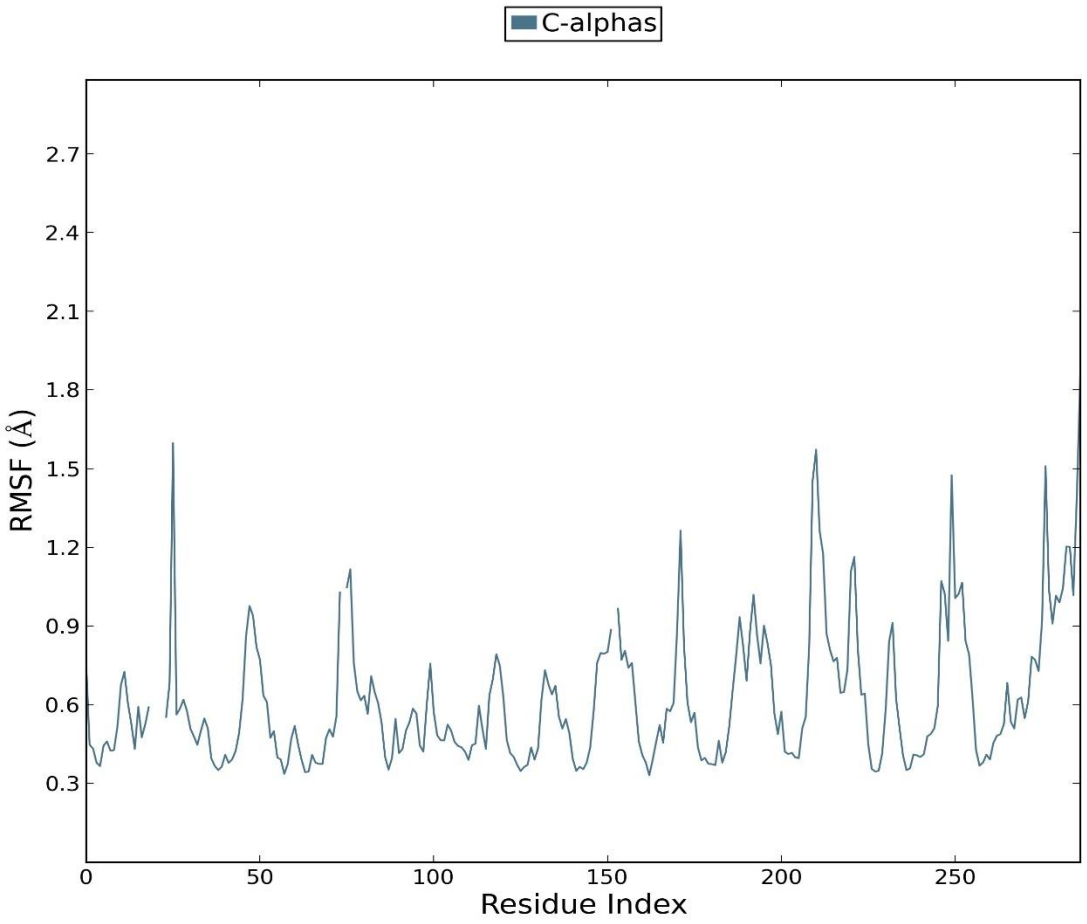

The Root Mean Square Fluctuation (RMSF) is useful for characterizing local changes along the protein chain and the ligand atom positions. Only six amino acids show high flexibility (Figure 5.25a) with the maximum value of 1.6 A^0. Throughout the process, the ligand V-2,4MEshows the flexibility in the range of 0.9-2.5 A^0 (Figure 5.25b). The $–O-CH_3$ group has higher flexibility with 2.5A^0.

Protein interactions with the ligand was monitored throughout the simulation. Most of the active site amino acids had hydrophobic interactions and Water Bridgesthan the Hydrogen Bonds and Ionic interactions (Figure 5.26).

Figure 5.25b: Root mean square fluctuations (RMSF) of o-vanillin V-2,4ME

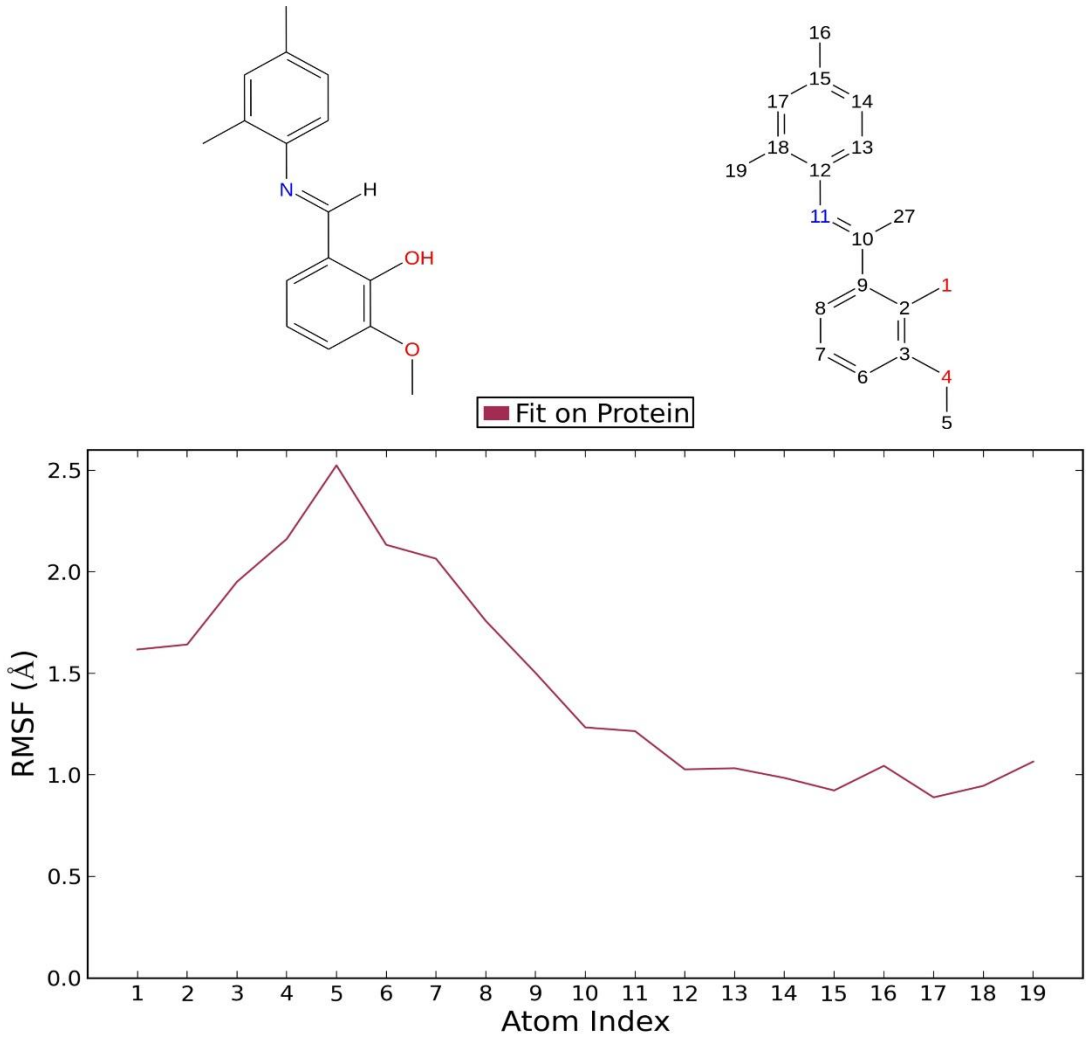

Figure 5.26: Interactions of Prothrombin (PDB ID: 3C1K) with V-2,4ME

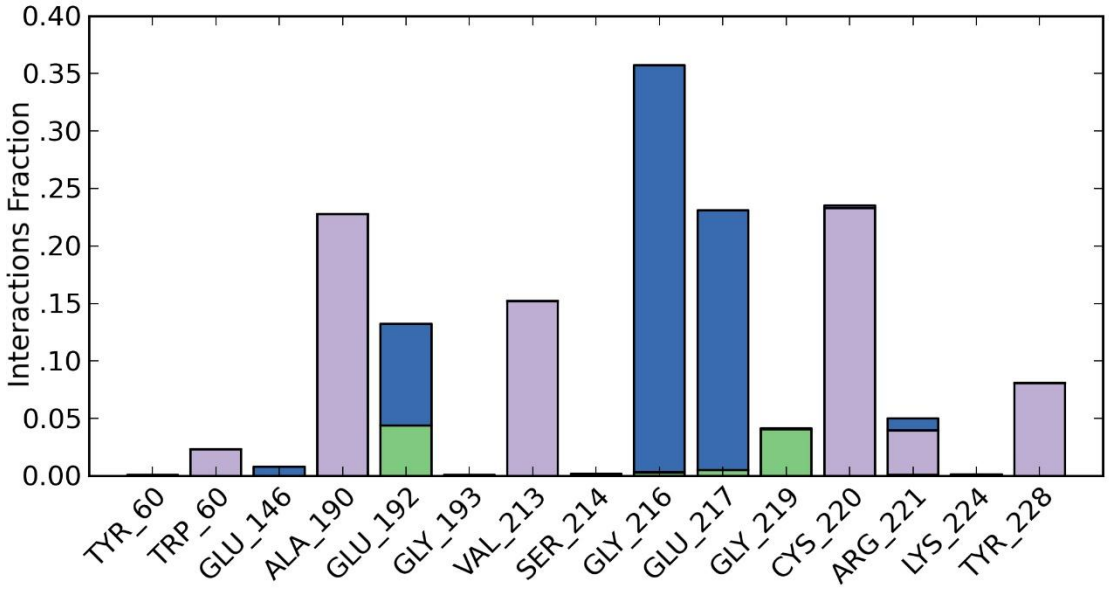

Figure 5.27: A timeline representation of the interactions and contacts (H-bonds, Hydrophobic, Ionic, Water bridges) between o-vanillin V-2,4ME and Prothrombin (PDB ID: 3C1K)

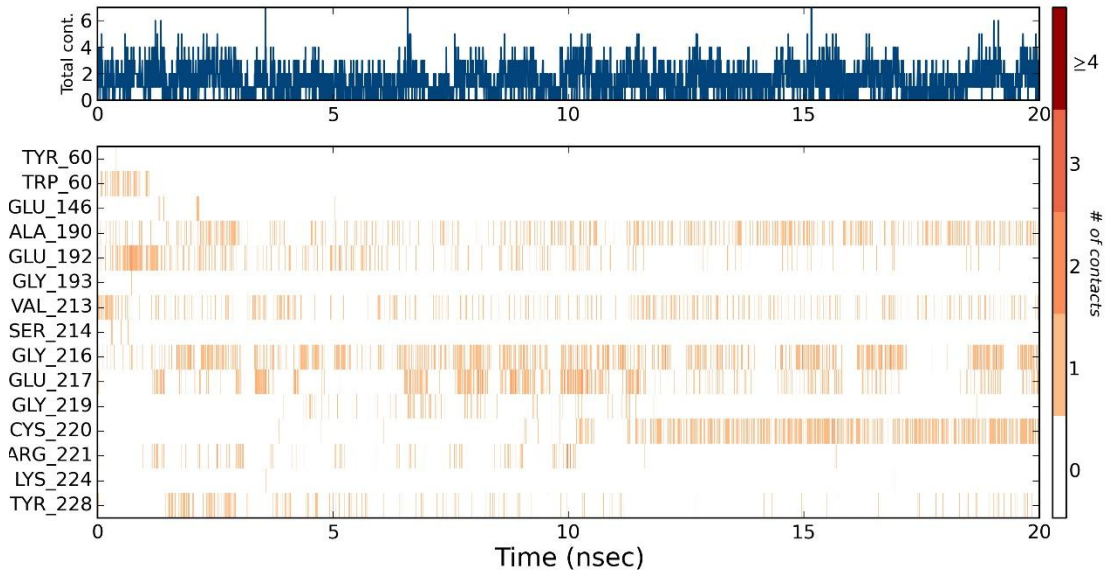

Figure 5.28: A schematic of detailed V-2,4ME atom interactions with the Prothrombin amino acid residues.

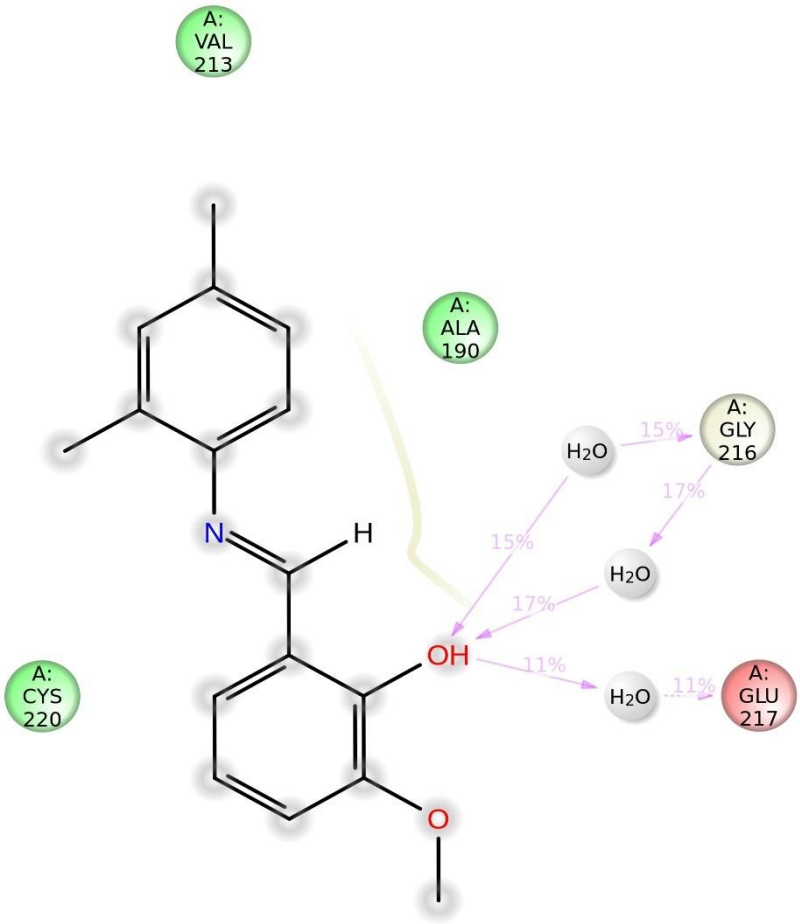

A timeline representation of the protein-ligand interactions and contacts summarized in figure 5.27. The top panel shows the total number of specific contacts the protein makes with the ligand over the course of the trajectory. The bottom panel shows which residues interact with the ligand in each trajectory frame. Some residues make more than one specific contact with the ligand, which is represented by a darker shade of orange, according to the scale to the right of the plot. The active site amino acids have interaction with ligand average of 3.4 ns (17% of 20 ns). Most of them, discontinuously contact the ligand. A schematic of detailed ligand atom interactions with the protein residues is shown in figure 5.28. The interactions that occur more than 10.0% of the simulation time in the selected trajectory (0.00 through 20.00 ns), are shown. The –OH group of ligand molecules contact the amino acid Glu 217 with one water molecule and Gly 216withtwo water molecules.

5.4 CONCLUSION

The current study adopted novel a ligand based approach in which the ligand information is available, but the biological activity is unknown. Various tools and databases were employed to identify the biological function of the synthesized acyl and aldehyde pyrazolone and O-vanillin derivatives. Finally, the binding mode of synthesized molecule with their predicted targets were studied by docking. The acyl pyrazolone derivatives PTPMP-EA, PMP-EA and MCPMP-EA were predicted and confirmed with its biological functions, which show anti-cancer, anti-inflammatory, anti-diabetes activity along with the inhibition of Hepatitis C Virus growth and Inactivation of estrogens. The aldehyde pyrazolone derivatives APTPMP-4BR, APTPMP-4F, APTPMP-3,4F and APTPMP-2,4ME were predicted and confirmed with its biological functions, which can help in autoimmune diseases, cancer treatment and as an immunosuppression agent. The O-vanillin derivatives V-4BR, MMM and V-2,4ME were predicted and confirmed with its biological functions, which can help in the controlling of methane production in the archaea and prevent blood coagulation by inhibiting prothrombin. The docking studies show the ligand molecules have better binding capacity with the respective proteins through hydrogen bond interaction. But, in the molecular dynamic studies reveals that, to understand the hydrogen bond interactions, the simulation time needs to be increased as poor hydrogen bonds are observed until 20 ns. The current study provides new insight to the synthetic chemist to predict the biological activity of novel molecules.

REFERENCES

374. C. Acharya, A. Coop, J.E. Polli, A.D. Mackerell, Jr., Current computer-aided drug design, 7 (2011) 10-22.

375. B.C. Duffy, L. Zhu, H. Decornez, D.B. Kitchen, Bioorganic & medicinal chemistry, 20 (2012) 5324-5342.

376. G. Landrum, J Cheminform, 5 (2013) 1-1.

377. A. Leach, J Cheminform, 3 (2011) 1-1.

378. D. Fourches, A. Tropsha, J Cheminform, 6 (2014) 1-1.

379. A.L. Hopkins, Nature chemical biology, 4 (2008) 682-690.

380. G.V. Paolini, R.H. Shapland, W.P. van Hoorn, J.S. Mason, A.L. Hopkins, Nature biotechnology, 24 (2006) 805-815.

381. E. Proschak, J Cheminform, 6 (2014) 1-1.

382. A. Koutsoukas, B. Simms, J. Kirchmair, P.J. Bond, A.V. Whitmore, S. Zimmer, et al., Journal of proteomics, 74 (2011) 2554-2574.

383. N. Wale, X. Ning, G. Karypis, Trends in Chemical Graph Data Mining, in: C.C. Aggarwal, H. Wang (Eds.) Managing and Mining Graph Data, Springer US, 2010, pp. 581-606.

384. L. Wang, X.Q. Xie, Future medicinal chemistry, 6 (2014) 247-249.

385. J.J. Georrge, V.V. Umrania, Applied biochemistry and biotechnology, 167 (2012) 1377-1395.

386. N. Vaishnav, A. Gupta, S. Paul, G. John, J Appl Genetics, (2014) 1-11.

387. J.J. Georrge, V. Umrania, Indian Journal of Biotechnology, 10 (2011) 432-439.

388. A. Sharma, P. Dutta, M. Sharma, N.K. Rajput, B. Dodiya, J.J. Georrge, et al., J Cheminform, 6 (2014) 46.

389. K. Rohitkumar, J.G. John, Life Sciences Leaflets, 62 (2015) 1-13.

390. A.R. Ali, E.R. El-Bendary, M.A. Ghaly, I.A. Shehata, European journal of medicinal chemistry, 75 (2014) 492-500.

391. J.M. Rollinger, D. Schuster, B. Danzl, S. Schwaiger, P. Markt, M. Schmidtke, et al., Planta medica, 75 (2009) 195-204.

392. V.A. Joseph, J.H. Pandya, R.N. Jadeja, Journal of Molecular Structure, 1081 (2015) 443-448.

393. J. V.A, K.M. Vyas, J.H. Pandya, V.K. Gupta, R.N. Jadeja, Journal of Coordination Chemistry, 66 (2013) 1094-1106.

394. J.H. Pandya, V.K. Gupta, R.N. Jadeja, Journal of the Indian Chemical Society, 89 (2012) 1-10.
395. v. LigPrep, in, LLC, New York, NY, 2005.
396. v. QikProp, in, LLC, New York, NY, 2009.
397. B. Hardy, N. Douglas, C. Helma, M. Rautenberg, N. Jeliazkova, V. Jeliazkov, et al., J Cheminform, 2 (2010) 7.
398. C. Qin, C. Zhang, F. Zhu, F. Xu, S.Y. Chen, P. Zhang, et al., Nucleic acids research, 42 (2014) D1118-1123.
399. N. Hecker, J. Ahmed, J. von Eichborn, M. Dunkel, K. Macha, A. Eckert, et al., Nucleic acids research, 40 (2012) D1113-1117.
400. M. Kuhn, D. Szklarczyk, S. Pletscher-Frankild, T.H. Blicher, C. von Mering, L.J. Jensen, et al., Nucleic acids research, 42 (2014) D401-407.
401. J. Gong, C. Cai, X. Liu, X. Ku, H. Jiang, D. Gao, et al., Bioinformatics, 29 (2013) 1827-1829.
402. C.G. Wermuth, C.R. Ganellin, P. Lindberg, L.A. Mitscher, in: Pure and Applied Chemistry, 1998, pp. 1129.
403. X. Liu, S. Ouyang, B. Yu, Y. Liu, K. Huang, J. Gong, et al., Nucleic acids research, 38 (2010) W609-614.
404. F.C. Bernstein, T.F. Koetzle, G.J. Williams, E.F. Meyer, Jr., M.D. Brice, J.R. Rodgers, et al., Archives of biochemistry and biophysics, 185 (1978) 584-591.
405. V. Law, C. Knox, Y. Djoumbou, T. Jewison, A.C. Guo, Y. Liu, et al., Nucleic acids research, 42 (2014) D1091-1097.
406. A. Gaulton, L.J. Bellis, A.P. Bento, J. Chambers, M. Davies, A. Hersey, et al., Nucleic acids research, 40 (2012) D1100-1107.
407. R. Thomsen, M.H. Christensen, J Med Chem, 49 (2006) 3315-3321.
408. M. Karplus, J.A. McCammon, Nat Struct Mol Biol, 9 (2002) 646-652.
409. Schrödinger Release 2013-1, in, Schrödinger, New York, NY, USA.
410. D. Shivakumar, J. Williams, Y. Wu, W. Damm, J. Shelley, W. Sherman, Journal of Chemical Theory and Computation, 6 (2010) 1509-1519.
411. R. Cascao, J. Polido-Pereira, H. Canhao, A.M. Rodrigues, M. Navalho, H. Raquel, et al., Clinical and experimental rheumatology, 30 (2012) 144.

412. M. Ramadani, F. Gansauge, S. Schlosser, Y. Yang, H.G. Beger, S. Gansauge, Journal of gastrointestinal surgery : official journal of the Society for Surgery of the Alimentary Tract, 5 (2001) 352-358.
413. G. Matute-Bello, Intensive care medicine, 33 (2007) 755-757.
414. A. Brik, C.H. Wong, Organic & biomolecular chemistry, 1 (2003) 5-14.
415. Y.C. Lin, M. Happer, J.H. Elder, Journal of virology, 87 (2013) 8524-8534.
416. H.A. Jung, Y.S. Cho, S.H. Oh, S. Lee, B.S. Min, K.H. Moon, et al., Archives of pharmacal research, 36 (2013) 957-965.
417. G. Scapin, S.B. Patel, J.W. Becker, Q. Wang, C. Desponts, D. Waddleton, et al., Biochemistry, 42 (2003) 11451-11459.
418. D. Shi, F. Xu, J. He, J. Li, X. Fan, L. Han, Chin. Sci. Bull., 53 (2008) 2476-2479.
419. D. Moradpour, F. Penin, C.M. Rice, Nature reviews. Microbiology, 5 (2007) 453-463.
420. V.J. Leveque, Q.M. Wang, Cellular and molecular life sciences : CMLS, 59 (2002) 909-919.
421. M.H. Powdrill, J.A. Bernatchez, M. Gotte, Viruses, 2 (2010) 2169-2195.
422. R.R. Deore, J.W. Chern, Current medicinal chemistry, 17 (2010) 3806-3826.
423. D.S. Goodsell, The oncologist, 11 (2006) 418-419.
424. D. Gschwantler-Kaulich, A. Fink-Retter, K. Czerwenka, G. Hudelist, A. Kaulich, E. Kubista, et al., Tumor Biol., 32 (2011) 501-508.
425. S. Liu, E.A. Neidhardt, T.H. Grossman, T. Ocain, J. Clardy, Structure, 8 (2000) 25-33.
426. K.C. Shih, C.C. Lee, C.N. Tsai, Y.S. Lin, C.Y. Tang, PloS one, 9 (2014) e87960.
427. S.F. Chen, R.L. Ruben, D.L. Dexter, Cancer research, 46 (1986) 5014-5019.
428. E.A. Kuo, P.T. Hambleton, D.P. Kay, P.L. Evans, S.S. Matharu, E. Little, et al., J Med Chem, 39 (1996) 4608-4621.
429. A. Veillette, N. Abraham, L. Caron, D. Davidson, Seminars in immunology, 3 (1991) 143-152.
430. E.F. DiMauro, J. Newcomb, J.J. Nunes, J.E. Bemis, C. Boucher, L. Chai, et al., J Med Chem, 51 (2008) 1681-1694.
431. J.B. Bolen, J.S. Brugge, Annual review of immunology, 15 (1997) 371-404.

432. J.H. Hanke, B.A. Pollok, P.S. Changelian, Inflammation research : official journal of the European Histamine Research Society ... [et al.], 44 (1995) 357-371.

433. J. Das, R.V. Moquin, J. Lin, C. Liu, A.M. Doweyko, H.F. DeFex, et al., Bioorganic & medicinal chemistry letters, 13 (2003) 2587-2590.

434. G. Jego, A. Hazoume, R. Seigneuric, C. Garrido, Cancer Lett, 332 (2013) 275-285.

435. J. Eskew, T. Sadikot, P. Morales, A. Duren, I. Dunwiddie, M. Swink, et al., BMC Cancer, 11 (2011) 1-16.

436. K. Sidera, E. Patsavoudi, Recent patents on anti-cancer drug discovery, 9 (2014) 1-20.

437. N. Wu, E.F. Pai, The Journal of biological chemistry, 277 (2002) 28080-28087.

438. N.J. Royle, D.M. Irwin, M.L. Koschinsky, R.T. MacGillivray, J.L. Hamerton, Somatic cell and molecular genetics, 13 (1987) 285-292.

439. R.C. Isaacs, M.G. Solinsky, K.J. Cutrona, C.L. Newton, A.M. Naylor-Olsen, D.R. McMasters, et al., Bioorganic & medicinal chemistry letters, 18 (2008) 2062-2066.

440. F. Claessens, G. Verrijdt, A. Haelens, L. Callewaert, U. Moehren, A. d'Alesio, et al., Andrologia, 37 (2005) 209-210.

441. E.P. Gelmann, Journal of clinical oncology : official journal of the American Society of Clinical Oncology, 20 (2002) 3001-3015.

442. S.-D. Yeh, P.-C. Yang, H.-H. Lu, C. Chang, C.-W. Wu, J Transl Med, 10 (2012) 1-2.

443. T. Sadowski, J. Steinmeyer, The Journal of rheumatology, 28 (2001) 336-340.

444. Y. Okamoto, H. Anan, E. Nakai, K. Morihira, Y. Yonetoku, H. Kurihara, et al., Chemical & pharmaceutical bulletin, 47 (1999) 11-21.

445. B.K. Biswal, M.M. Cherney, M. Wang, L. Chan, C.G. Yannopoulos, D. Bilimoria, et al., The Journal of biological chemistry, 280 (2005) 18202-18210.

446. S. Shevtsov, E.V. Petrotchenko, L.C. Pedersen, M. Negishi, Environmental health perspectives, 111 (2003) 884-888.

447. V.A. Joseph, J.H. Pandya, R.N. Jadeja, Journal of Molecular Structure, 1081 (2015) 443-448.

448. L. Wright, X. Barril, B. Dymock, L. Sheridan, A. Surgenor, M. Beswick, et al., Chemistry & biology, 11 (2004) 775-785.